

## Sequence stratigraphic controls on early-diagenetic carbonate cementation of shallow marine clastic sediments (the Devonian Zakeen Formation, southern Zagros, Iran)

Seyed Mohammad Zamanzadeh\* School of Geology, University college of Science, University of Tehran, Tehran, Iran  
Faculty of Geography, University of Tehran, Tehran, Iran  
Abdolhossein Amini School of Geology, University college of Science, University of Tehran, Tehran, Iran  
Mohammad Ghavidel-Syooki Exploration Directorate, National Iranian Oil Company, Hafez Crossing, Taleghani Avenue, Tehran, Iran

**ABSTRACT:** Distribution pattern of carbonate cements of the Middle to Upper Devonian Zakeen Formation of southern Zagros, suggests a close relationship between relative sea-level changes and diagenetic processes. Ferroan dolomite cementation is closely linked to genetically related facies (parasequences, systems tracts, sequences) and/or major stratal surfaces (transgressive and maximum flooding surfaces and sequence boundaries). The cements are systematically distributed within the lowstand, transgressive and highstand systems tracts. Eogenetic ferroan dolomite cement ( $^{18}\text{O}$  from 1.06 to  $-6.00\%$  VPDB and  $^{13}\text{C}$  from  $-1.23$  to  $-4.94\%$  VPDB) was developed in the form of: 1) ferroan dolomite cemented conglomerates in LST estuarine environments, 2) laterally extensive ferroan dolomite cemented sandstones in LST estuarine and TST foreshore-shoreface environments and along maximum flooding surfaces and 3) ferroan dolomite cemented nodules in LST, TST and HST foreshore-shoreface environments. Prolonged subaerial exposure of the strata, resulted from epeirogenic movements of the Hercynian Orogeny, is considered to be responsible for cement and grains leaching and porosity development in sandstones underlying the major sequence boundary at the top of the Zakeen Formation.

**Key words:** sequence stratigraphy, Zagros, ferroan dolomite, Iran

### 1. INTRODUCTION

Investigating diagenetic processes in a sequence stratigraphic framework has recently gained significant interest and has been predominantly applied to carbonate successions (e.g., Read and Horbury 1993; Tucker 1993; Moss and Tucker 1996). From the last decade onward relationships between diagenetic processes and sea-level fluctuations in clastic rocks have increasingly been gaining attentions (e.g., Tang et al., 1994; Amorosi 1995, 1997; Taylor et al., 1995, 2000; Loomis and Crossey 1996; Dutton and Willis 1998; South and Talbot 2000; Ketzer et al., 2002; Al-Ramadan et al., 2005). However, the relationship between diagenetic processes and sea-level fluctuations are not adequately investigated yet (Ketzer et al., 2003). Among the various aspects

of diagenetic features in siliciclastic rocks, the distribution of carbonate cements and clay minerals in relation to sea-level changes have received the greatest attention (e.g., Taylor et al., 1995; McKay et al., 1995; Morad et al., 2000; Ketzer et al., 2002, 2003; Worden and Morad 2003). Development of early diagenetic carbonate cements has been attributed to: (1) long-term residence of deposits at sediment-water interface and low sedimentation rate (Taylor et al., 1995; Ketzer et al., 2003), (2) the formation of carbonate concretions along marine flooding surfaces (Loomis and Crossey 1996) and (3) extensive carbonate cements precipitation along parasequence boundaries (Ketzer et al., 2002). Distribution of eogenetic clay minerals (e.g., kaolinite, smectite, palygorskite, glauconite and berthierine), mechanically infiltrated clays, and clay-rich mud intraclasts has been discussed in a sequence stratigraphic framework to some extent (e.g., Worden and Morad, 2003; Ketzer et al., 2003).

In this paper, the relationship between development of carbonate cements and fluctuation of sea level in the Middle to Upper Devonian Zakeen Formation of the Zagros area, Iran is investigated. This formation is one of the most important siliciclastic units in the area and is under investigation for its hydrocarbon reservoir capability. It lies on the top of Silurian shale (Sarchahan Formation) which has been considered as a major source rock in the area (Kashfi, 1992; Kamali and Rezaee, 2003). It unconformably lies under the Lower Permian Faraghan Formation (equivalent to the upper Unayzah Formation in Saudi Arabia) which grades into the Middle to Upper Permian Dalan and Lower Triassic Kangan formations. The last two formations are known as main reservoirs of the Southern Pars giant gas field (Aali et al., 2006). Regardless of its importance in the Zagros stratigraphy, only minor information on the sedimentary petrology, depositional environment, and sequence stratigraphy of the Zakeen Formation is available. Nevertheless, detailed palynological studies have resulted in precise biozonation and age determination of the Zakeen Formation

\*Corresponding author: smzamazadeh@gmail.com

and identification of a significant hiatus (almost 80 million years) between the Zakeen and overlying Faraghan formations (Ghavidel-Syooki, 1986, 1997, 1999, 2003). This paper as part of a large project which investigates sedimentary petrology, depositional environment, and sequence stratigraphy of the Zakeen Formation in the South Zagros area (Zamanzadeh 2008), concentrates on the associations of sequence stratigraphy and major diagenetic features.

2. GEOLOGICAL SETTING

This study was carried out on excellent exposures of the Zakeen Formation in Gahkum Mountain, which is part of High Zagros zone located 120 km north of Bandar Abbas City at 28°05'12"N, 55°56'50"E (Fig. 1).

In terms of tectonic setting, the study area is part of the High Zagros zone (Berberian and King 1981). The High Zagros zone comprises several thrust faults, one of which has juxtaposed Paleozoic rocks against Mesozoic and Cenozoic rocks and provided excellent outcrops of Lower Paleozoic to Triassic successions. During the late Palaeozoic the area was part of the Arabian Platform (Beydoun 1988), located at southern margins of the Neo-Tethys Ocean, at latitudes of about 30° to 45° south (Berberian and King 1981; Smith et al., 1981; Hussein 1992; Konert et al., 2001; Zharkov

and Chumakov, 2001).

The Middle to Upper Devonian (Ghavidel-Syooki, 2003) Zakeen Formation unconformably overlies the Early Silurian Sarchahan Formation and underlies the Lower Permian Faraghan Formation in the study area. The Sarchahan Formation is characterized by alternations of thick shales and thin lenses of sandstone/conglomerate. The Zakeen Formation is bounded by distinct unconformities above and below (Fig. 1). The lower unconformity seems to be the result of Upper Silurian and Lower Devonian hiatuses produced by extensive erosion in the study area and exposures are produced by local folding and faulting (Ghavidel-Syooki 2003; Konert et al., 2001). The upper unconformity represents Upper Devonian hiatus which was generated by the Hercynian (Variscan) Orogeny and glaciation in Gondwana during the Carboniferous (McGillivray and Hussein, 1992; Konert et al., 2001). The Zakeen Formation (the time-equivalent to the Jauf and Jubah formations in Saudi Arabia) is characterized by alternating layers of cross-stratified sandstone, conglomerate and thin lenses of mudstone in the study area. The Lower Permian (Ghavidel-Syooki 1997, 1999, 2003) Faraghan Formation (the time-equivalent to the Upper Unayzah Formation in Saudi Arabia) is dominated by cross-stratified sandstone and about 15 meters of stromatolitic dolomite near the base. The formation grades into Middle to Upper

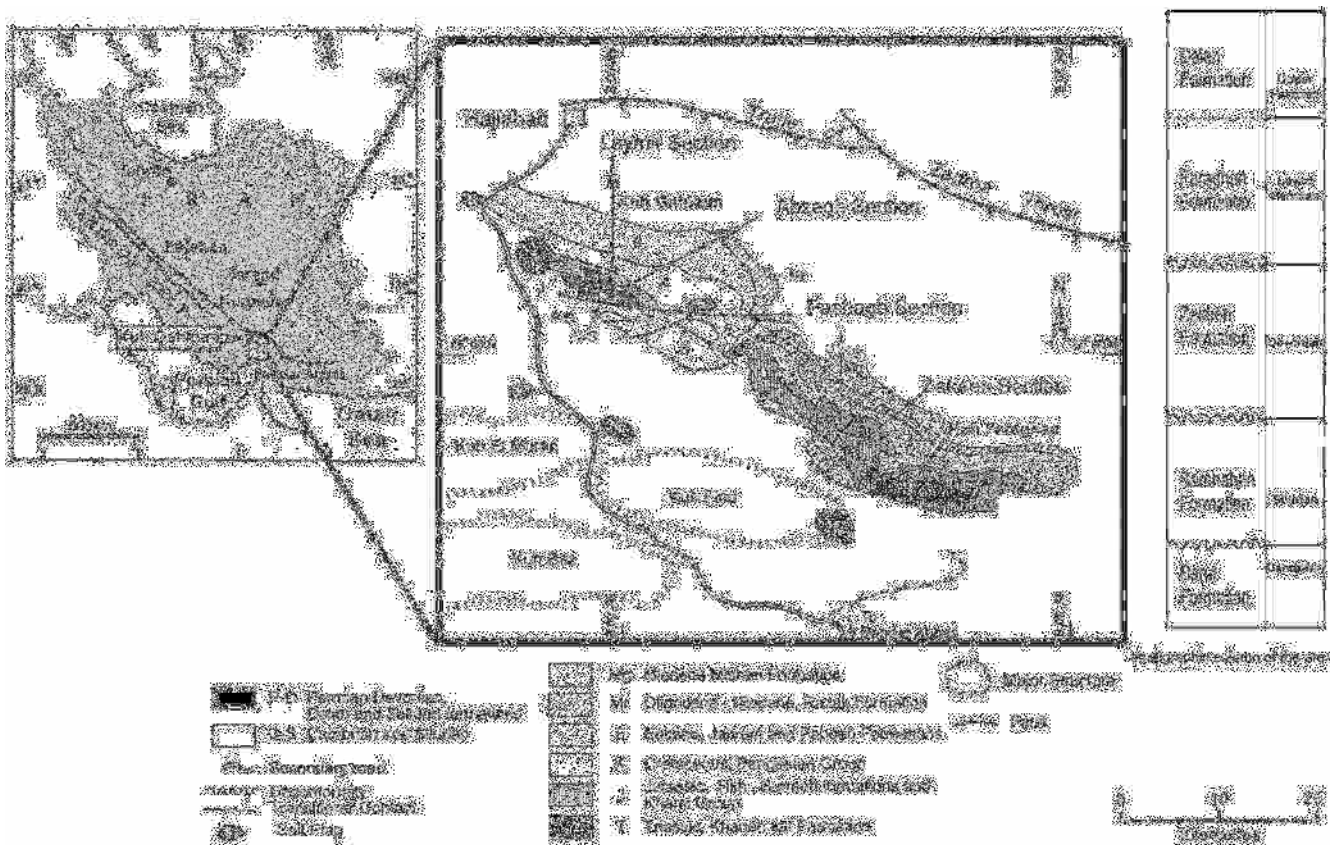


Fig. 1. Location map of the studied area (modified from Ghavidel-Syooki and Winchester-Seeto, 2004).

Permian Dalan carbonates (time equivalent of the Khuff Formation in Saudi Arabia). Similar to the other parts of Middle East, the upper Paleozoic sedimentation in Iran took place in a shallow marine environment (Berberian and King 1981; Al-Sharhan and Nairn 1997, Zamanzadeh 2008) during Devonian time, in which the globe experienced warm climatic conditions (Frakes et al., 1992).

### 3. METHODOLOGY

Lithofacies and petrofacies analysis of the Zakeen Formation in several outcrops (Zakeen, Abzagh, Laymir and Pashagh sections) (Fig. 1) resulted in selection of the Abzagh Section of Gahkum Mountain for the study of major diagenetic features in a sequence stratigraphic framework.

Excellent exposures of the Zakeen Formation, variety of its constituent facies and its substantial lateral extent, good exposures of the overlying Faraghan and Dalan and underlying Sarchahan formations, and gentle structural deformation of the area were main reasons for such a selection. Description of lithology, sedimentary structures, fossil content, geometry, paleocurrent pattern and the nature of stratal surfaces (Miall, 1985) led to the identification of the major lithofacies. In this regard, 11 lithofacies were determined and described (Table 1). A total of 155 rock samples were collected, mainly based on lithological variations, for petrofacies analysis, diagenetic studies, geochemical and other laboratory measurements.

Table 1. General description of major lithofacies and their constituent petrofacies/microfacies

Lithofacies	General description	Petrofacies/ microfacies	Description
Gm	Pebble-size, massive or crudely stratified, poorly sorted, sub-mature ortho-conglomerate. Lenticular geometry and erosional scoured base. Occurs at the base of fining-up sequences. Marked by abundant mud rip-up clasts.	(OG) Orthoconglomerate	Ferroan dolomite cemented, poorly sorted, extrabasinal, polymictic orthoconglomerate. Carbonate, sandstone and shale lithics and chert grains are dominant framework constituents. The sandy matrix is dominated by quartz with minor feldspar grains. Some carbonate lithics show characteristics of stromatolite and bindstone. Phosphatic pebbles are locally observed.
Gp	Pebble-size, planar cross-stratified (crude), rip-up mud clast bearing, moderately sorted sub-mature, ortho-conglomerate. Wide lenticular geometry and erosional scoured base. Associated with Sr lithofacies	(PG) Paraconglomerate	A matrix supported (dolomite to dolomicrite are common matrix) extrabasinal, polymictic, paraconglomerate. Carbonate cement (recrystallized matrix) is locally observed. Chert grains carbonate, sandstone, shale and muddy lithics are dominant framework constituents. Some anhydrite patches are observed within the carbonate matrix.
St	Low angle cross-stratified, moderate to well-sorted sandstone. Wide lenticular to sheet-like geometry and abundant reactivation surfaces. Marked by sharp lower and transitional upper contacts. Comprising heavy mineral horizons.	(QA) Qarenite	Siliceous and ferroan dolomite cemented, well sorted, texturally and mineralogically mature, fine to coarse grain quartz arenite. Clayey cements (chlorite, illite-sericite) are locally observed as pore linings. Dolomite occurs as poikilotopic cement in places. It is marked by high fracturing of the framework grains. Phosphotized shell fragments are locally observed. In places the petrofacies is burrowed and filled with phosphatic matrix. Overgrowth Si cement is also common.
Sp	Planar cross stratified, moderate to well sorted, sub-mature to mature, pebbly sandstone. Wide lenticular to sheet-like geometry, with erosional base in places. Some herring-bone structures and dolomite patches are observed.	(FA) Feldspathic arenite	Siliceous and ferroan dolomite cemented, moderately sorted, texturally and mineralogically sub-mature, fine to medium grain feldspathic arenite. The feldspar content rarely exceeds 20%, although few arkosic rocks are observed. Illite-sericite, chlorite, sericite, and phosphate occur as minor cement in the petrofacies. Chlorite is common clay occurs in special horizons in places (depositional clay)
Sr	Ripple cross-laminated, moderate to poorly sorted, sub-mature sandstone. Wide lenticular to sheet-like geometry, highly associated with lithofacies Sh, Sl and Sm.	(QW) Quartzwacke	It is characterized by a carbonate matrix (dominantly dolomite), in which unsorted and angular quartz grains are scattered (matrix supported). Carbonate lithics are minor constituent of the framework. The petrofacies is characterized by textural inversion (mineralogically mature and texturally immature) in most places.
Sl	Low angle cross stratified sandstone/silty sandstone. Wide lenticular to sheet-like geometry. Abundant reactivation surfaces and rip-up mud clasts. Both erosional and sharp contacts are observed. Highly associated with ripple cross-laminated sandstones.		

Table 1. (continued)

Lithofacies	General description	Petrofacies/ microfacies	Description
Sm	Poorly sorted, immature to sub-mature massive sandstone with abundant carbonate content (hybrid in nature). Marked by erosional base and abundant mud/carbonate pockets (flaser-bedding appearance). Wide lenticular geometry. Local hummocky and swaley structures.	(SLA) Sublitharenite	Ferroan dolomite to dolomite cemented, moderately to poorly sorted, texturally sub-mature, and mineralogically immature, fine to medium grain sublitharenite. Carbonate lithics are dominant constituents of the framework. The petrofacies is characterized by high (~10%) matrix content which seems to be pseudomatrix (Dickinson 1970). Phosphate occurs as minor cement in places. Phosphatic shell fragments are also presented.
Fl	Finely laminated fissile siltstone/sandy siltstone. Some soft sediment deformations and rip-up mud clasts are observed. Sheet-like geometry with gradational contacts.	(Sz) Siltstone	Ferroan dolomite and chlorite cemented micaceous to calcareous siltstone/sandy siltstone. Unsorted fine-sand to silt-size quartz grains are scattered in a muddy background (carbonate matrix). It is marked by abundant micas. Dolomitization of carbonates occurs in places. Fracture filled carbonate cement is common.
		(Ss) Sandy shale	Physil (more than 50% clay content) shale with minor sand-size grains (Quartz, feldspar, carbonate lithics). The background is dominantly calcareous, and illite is dominant clay determined by X-ray diffractometer.
Dm	Thick bedded, massive dolomite to dolomudstone with rusty appearance. Marked by abundant desiccation cracks and scattered patches of anhydrite/gypsum. Sheet-like geometry and sharp contacts.	(DI) Dolostone	Large crystalline anhedral to subhedral neomorphic dolomite. Dolomitization has either destructively occurred, so that previous carbonate constituents (e.g., intraclasts, ooids and peloids) are not distinguished, or it was less severe and the ghosts of grains are visible. Some phosphatic grains are observed. Sometimes zoned, saddle dolomite and megacrystals of calcite cement are observed.
M	Limestone to calcareous mudstone. Abundant reactivation surfaces and shell fragments (some fish debris). Sheet-like geometry and sharp contacts. Highly associated with lithofacies Fl, Sh, and Sm.	(Md) Mudstone	Calcareous mudstone (physilitic) to micrite.

To examine the volume and distribution of porosity, 80 blue-dyed impregnated thin sections were prepared. The volume of cement was determined by point counting (300 points per thin section) in the specimens which were completely cemented by ferroan dolomite. For petrofacies analysis of the rocks, petrographic techniques and SEM analysis were applied. In this regard, 10 petrofacies were determined (Table 1). To distinguish the mineralogy of carbonate cements, 20 sandstone samples (quartzarenites and subarkoses) with carbonate cements were selected, powdered and subjected to XRD analysis using a Siemens D5000 X-ray diffractometer. Combination of results from lithofacies and petrofacies analysis (Table 1) resulted in discrimination of 11 depositional facies (Table 2).

A Zeiss DSM 960A scanning electron microscope (SEM) was used to investigate crystal habits and textural relationships. Oxygen and carbon isotope analyses of carbonate cements were performed on seven samples which were collected along major stratal surfaces. Since there were no bioclastic grains and the cement homogeneously filled all the voids in sandstones, specimens were prepared by powder-

ing of carbonate cemented quartz arenites (bulk samples). Dolomite-cemented samples were reacted with 100% phosphoric acid at 50 °C for 24 hours. Samples containing both calcite and dolomite were subjected to sequential chemical separation treatment (Al-Aasm et al., 1990). The analyses were performed using a Thermo Finnigan mass spectrometer. Precision for all analyses was better than  $\pm 0.1\%$ . The oxygen and carbon isotope data are presented in the delta notation relative to the Vienna PDB. Classification of diagenetic products into eogenetic or mesogenetic stage is based on Morad et al. (2000).

#### 4. DEPOSITIONAL FACIES AND SEQUENCE STRATIGRAPHY

##### 4.1. Sedimentology

On the basis of lithological characteristics, sedimentary structures, geometry, fossil content, and stratal surfaces and also comparison with sediments from well known environments (e.g., Miall, 1999; Walker, 1992; Reading, 1996; Selley,

Table 2. General description of major facies and their depositional environment

Facies	Lithofacies/petrofacies or microfacies	Depositional environment
Z <sub>1</sub>	Gp/OG (Table 1) It is marked by high matrix content (~15%) in places.	Deposition by unidirectional currents in subaqueous channels of foreshore sub-environment. They show characteristics of longitudinal bars of in channels and mouth bars of channel inlets.
Z <sub>2</sub>	Gm/PG (Table 1)	Deposition by rapidly waning flow regime (unidirectional currents) in a subaqueous channel or a shallow marine siliciclastic shelf, which was marked by high fluctuation of sea level change and high sediment supply from the land.
Z <sub>3</sub>	Sl/FA and SA (Table 1)	Deposition by low flow regime unidirectional traction currents (longshore currents) in the shoreface sub-environment of a shallow marine shelf.
Z <sub>4</sub>	Sm/SLA, QW and HB (Table 1).	Rapid deposition in the offshore-transition sub-environment of a siliciclastic shelf during storm stages and high sediment supply to the basin.
Z <sub>5</sub>	Sp/QA and SA (Table 1).	Deposition in foreshore sub-environment of a shallow marine siliciclastic shelf and/or proximal part of the shoreface with significant long-shore currents.
Z <sub>6</sub>	St/QA (Table 1). Heavy mineral horizons are diagnostic.	Deposition in a relatively high energy setting by unidirectional currents. Distributary channels of foreshore (beach) to shoreface sub-environments of a shallow marine siliciclastic shelf, in periods of high sediments supply from the land.
Z <sub>7</sub>	Sh/FA and SLA and QW (Table 1).	Deposition in the bays and/or estuaries of a shallow marine siliciclastic shelf. In the shoreface or offshore transition sub-environments during calm stages (low sediment supply to the basin).
Z <sub>8</sub>	Sr/QW and HB (Table 1).	Deposition by low flow regime unidirectional traction currents in the upper shoreface sub-environment or by oscillatory currents in vicinity of fair weather wave base during calm stages.
Z <sub>9</sub>	Fl/Sz and Ss (Table 1).	Distal part of offshore-transition to proximal offshore sub-environments.
Z <sub>10</sub>	M/Md (Table 1).	Development in the bays, estuaries and/or offshore sub-environment of a clastic shelf during low sediment supply and/or relative sea level rise.
Z <sub>11</sub>	Dm/Do (Table 1).	Deposition in the supratidal sub-environment of a shallow marine system during low sediment supply periods.

1996), the major facies are determined. The distinguished facies of the Zakeen Formation are classified as Z<sub>1</sub> to Z<sub>11</sub> (Table 2). These facies as a whole represent sedimentation in a shallow marine environment. The depositional environment includes estuary, bay, foreshore with tidal channels, shoreface and offshore subenvironments (Reading, 1996). Each subenvironment can be distinguished by specific facies associations, the descriptions of which are followed. Sedimentation in the shelf, where estuaries and bays were common sub-environments, was mainly controlled by fluvial processes. The shelf environment has most likely experienced large fluctuations of base-level changes (Catuneanu 2002), the result of which is recorded as progradational and retrogradational sequences.

#### 4.1.1. Estuarine facies association

Erosionally-based, fining-upward succession passes from conglomerate (facies Z<sub>1</sub> and Z<sub>2</sub>) to sandstones with abundant cross stratifications (facies Z<sub>3</sub>, Z<sub>5</sub>, Z<sub>6</sub> and Z<sub>8</sub>) to mudstones (facies Z<sub>11</sub> and Z<sub>9</sub>) with mud cracks at the top. The conglomerate and sandstone facies (Z<sub>1</sub>, Z<sub>2</sub>, Z<sub>3</sub>, Z<sub>5</sub>, Z<sub>6</sub> and Z<sub>8</sub>) are marked by abundant phosphatic fish debris and heavy minerals. The conglomerates in this facies association represent the events of incision of the lower strata by fluvial activity and later channel fill.

#### 4.1.2. Bay facies association

This facies association is composed of fining-upward, medium- to coarse-grained cross-stratified to massive sandstones (facies Z<sub>3</sub>, Z<sub>4</sub>, Z<sub>5</sub>, Z<sub>6</sub>, Z<sub>7</sub> and Z<sub>8</sub>) which grade upward to green shale or sometimes carbonate mudstone (facies Z<sub>9</sub> and Z<sub>10</sub>). The sandy facies are marked by abundant heavy minerals and mudclasts. Conglomeratic beds (facies Z<sub>1</sub> and Z<sub>2</sub>) are rarely observed at the base of succession.

#### 4.1.3. Foreshore facies association

This facies association is composed of wide lenticular medium- to coarse-grained, well-sorted, cross-stratified to massive sandstones (facies Z<sub>3</sub>, Z<sub>4</sub>, Z<sub>5</sub>, Z<sub>6</sub>, Z<sub>7</sub> and Z<sub>8</sub>). The facies is characterized by various reactivation surfaces, abundant heavy minerals, and phosphatic fish debris. Some conglomeratic facies (less than 30 centimeters thick, facies Z<sub>1</sub>) channel fills are locally observed, which are ascribed to a tidal channel deposit. This conglomeratic facies is immediately followed by the above mentioned cross-stratified sandstones (especially Z<sub>3</sub>, Z<sub>5</sub>, Z<sub>6</sub>, Z<sub>7</sub> and Z<sub>8</sub>). Toward the top of the formation sabkha environment facies, which is represented by sabkha type micro-dolomites (facies Z<sub>11</sub>), is observed. The thickness of these dolomite layers does not exceed one meter.

#### 4.1.4. Shoreface facies association

This facies association occurs as fining-upward successions made up of medium-grained, massive to cross-stratified sandstones (facies Z3, Z4 and Z7) interbedded with siltstone and green sandy shale (facies Z9). Pyrite nodules are common in the shaley facies. The sandy facies shows hummocky and swaley cross-stratifications and contain phosphatic fish debris and phosphate-cemented siltstone fragments.

#### 4.1.5. Offshore facies association

This facies association is a laterally extensive body of rocks composed of sandy shales and siltstone or sometimes carbonate mudstone (facies Z9 and Z10) and interbedded fine-grained massive to cross-stratified sandstone (facies Z3 and Z4). Its component facies are characterized by the presence of pyrite minerals and some phosphatic fish debris.

### 4. 2. Sequence Stratigraphy

The whole formation shows a progradational stacking pattern (shallowing upward) (Fig. 2), which indicates an overall relative sea-level fall during the Middle to Upper Devonian, similar to other parts of the Arabian Plate and the world (Vail et al., 1977; Al Laboun, 1990). This relative sea-level fall resulted in extensive exposure in the study area during the Carboniferous, the result of which is recorded as an 80 million-year hiatus in the South Zagros area (Ghavidel-Syooki, 1997, 1999, 2003). Occurrence of the Lower Permian Faraghan Formation over the Zakeen Formation indicates the least exposure and erosion compared to other parts of the Zagros where the Faraghan Formation overlies rocks not younger than the Silurian (Szabo and Kheradpir, 1978, Ghavidel-Syooki, 1997, Alavi, 2004).

On the basis of facies characteristics (lithofacies and petrofacies analyses) and their environmental conditions, stratigraphic positions of the facies and their ordering in the measured section, and results from previous palynological studies (Ghavidel-Syooki, 1997, 1999, 2003), constituent sequences of the formation were determined and described (Zamanzadeh, 2008). Major building blocks of the sequences (systems tracts) and their stratal surfaces (dominantly sequence boundary and maximum flooding surface) were investigated using the following parameters.

Apart from the sedimentological characteristics of the facies, distinct erosional surfaces at the base of channel-fill deposits along with calcrete nodules, soil horizons, Fe-oxide cementation, development of mud cracks and mud rip-up clasts, and brecciation were the major indicators used for sequence boundary determination.

Development of phosphate and carbonate cements, occurrence of glauconite in the rocks, bioturbation, development of marine erosion (ravinement), and condensed sections (low rate of sedimentation) are indicators used for determination

of transgressive surface and maximum flooding surface.

The lowstand systems tract (LST) occur in the form of incised valley fills, development of supra-tidal deposits, and reworking of supra-tidal to shoreface sediments (Fig. 2).

The fining-upward packages of facies represent a gradual passage from foreshore/supratidal to shoreface/offshore deposits and indicate a transgressive systems tract (TST) in most places. Abundant bay and estuary deposits along with minor distributary channels and land-derived facies are other characteristics of this systems tract. This systems tract is associated with condensed sections (low rate of sedimentation) and marine erosion surfaces.

The highstand systems tract (HST) in the study area is marked by dominance of foreshore and shoreface facies in a coarsening-up (progradational) pattern. Due to large fluctuations of sea-level and sediment supply this systems tract is dominantly composed of the superimposed parasequences with distinct erosional surfaces. Forced regressive systems tract (FRST) deposits are rarely observed in the studied section. These deposits occur as sub-aqueous fans/turbidites developed during the relative sea-level fall, mostly in the shoreface and offshore sub-environments. Reworking of supratidal deposits (dolomites) and their deposition as intraclasts along with shoreface deposits are other characteristics of this systems tract. Based on the nature of stratal surfaces (especially sequence boundaries), the nature of facies ordering, thickness and the age of formation and its biozonation (Ghavidel-Syooki, 1997, 1999, 2003), the sequences were classified into three groups (2<sup>nd</sup>, 3<sup>rd</sup>, and 4<sup>th</sup> to 5<sup>th</sup> order sequences) (Fig. 3).

### 5. DISTRIBUTION OF DIAGENETIC MINERALS

Dolomite (dominantly ferroan), kaolinite, chlorite, illite-sericite, phosphate, glauconite, quartz and feldspar overgrowths are diagenetic minerals observed in the Zakeen Formation. On the basis of petrographic studies and SEM observations, the paragenetic sequence of the diagenetic products is constructed (Zamanzadeh, 2008) (Fig. 4).

These diagenetic minerals are categorized as products of eogenetic (e.g., ferroan dolomite and phosphate) and mesodiagenetic (e.g., saddle and zoned dolomite, chlorite, illite-sericite coatings and quartz and feldspar overgrowths) stages.

#### 5.1. Dolomite Cement

This cement occurs in the forms of sabkha-type micro/fine crystalline dolomite and microcrystalline ferroan dolomite. The ferroan dolomite dominantly occurs as microcrystalline and zoned sub-euhedral forms (Fig. 5). Saddle dolomite (mesogenetic) filling the fractures and voids of conglomerates is locally observed. In terms of geometry, the ferroan dolomite is stratabound in the sandstones, and occurs as laterally extensive layers in the conglomerates

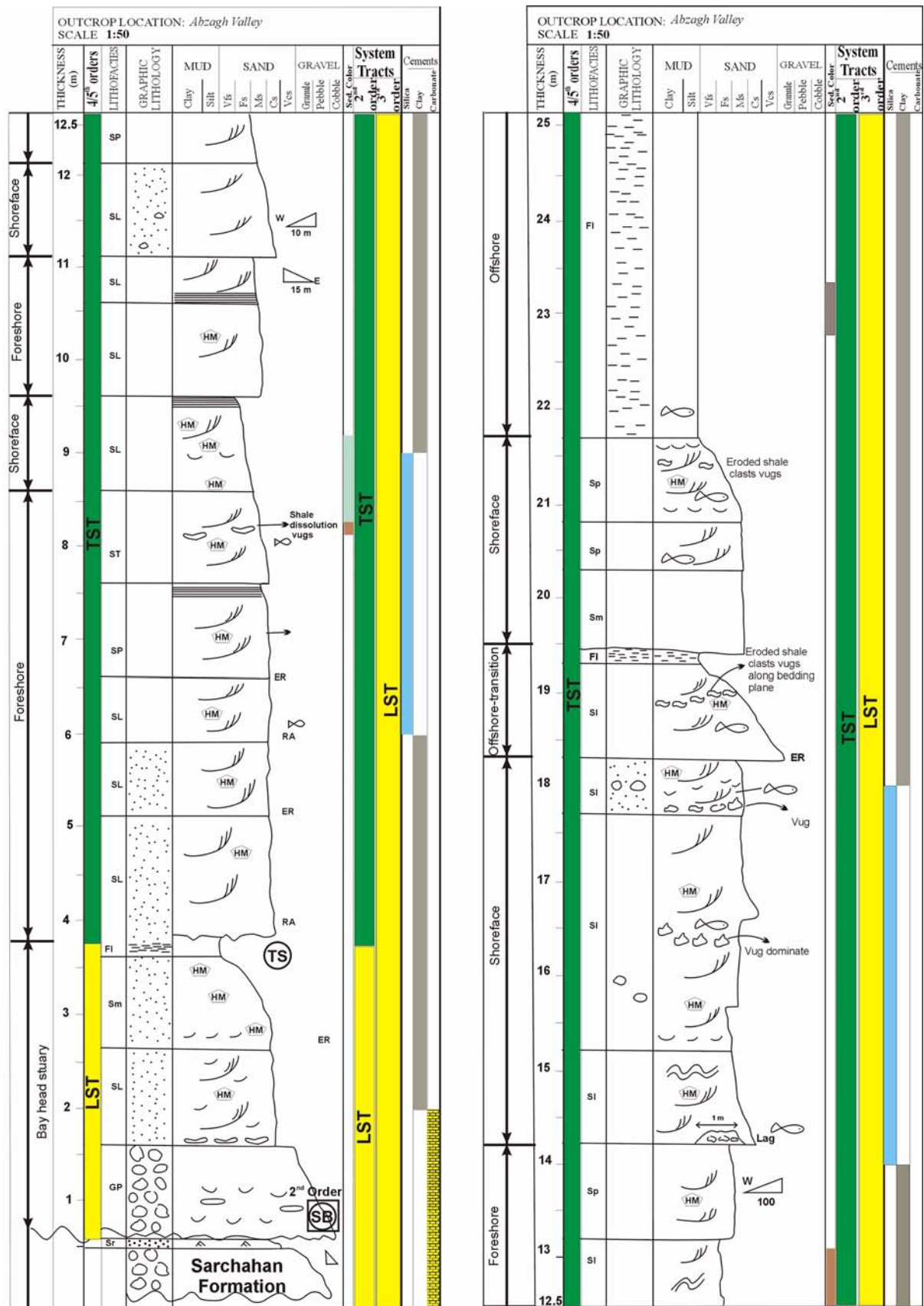


Fig. 2. Sedimentological logs of the studied formations illustrating the distribution of major building blocks (systems tracts) and the nature of constituent sequences.



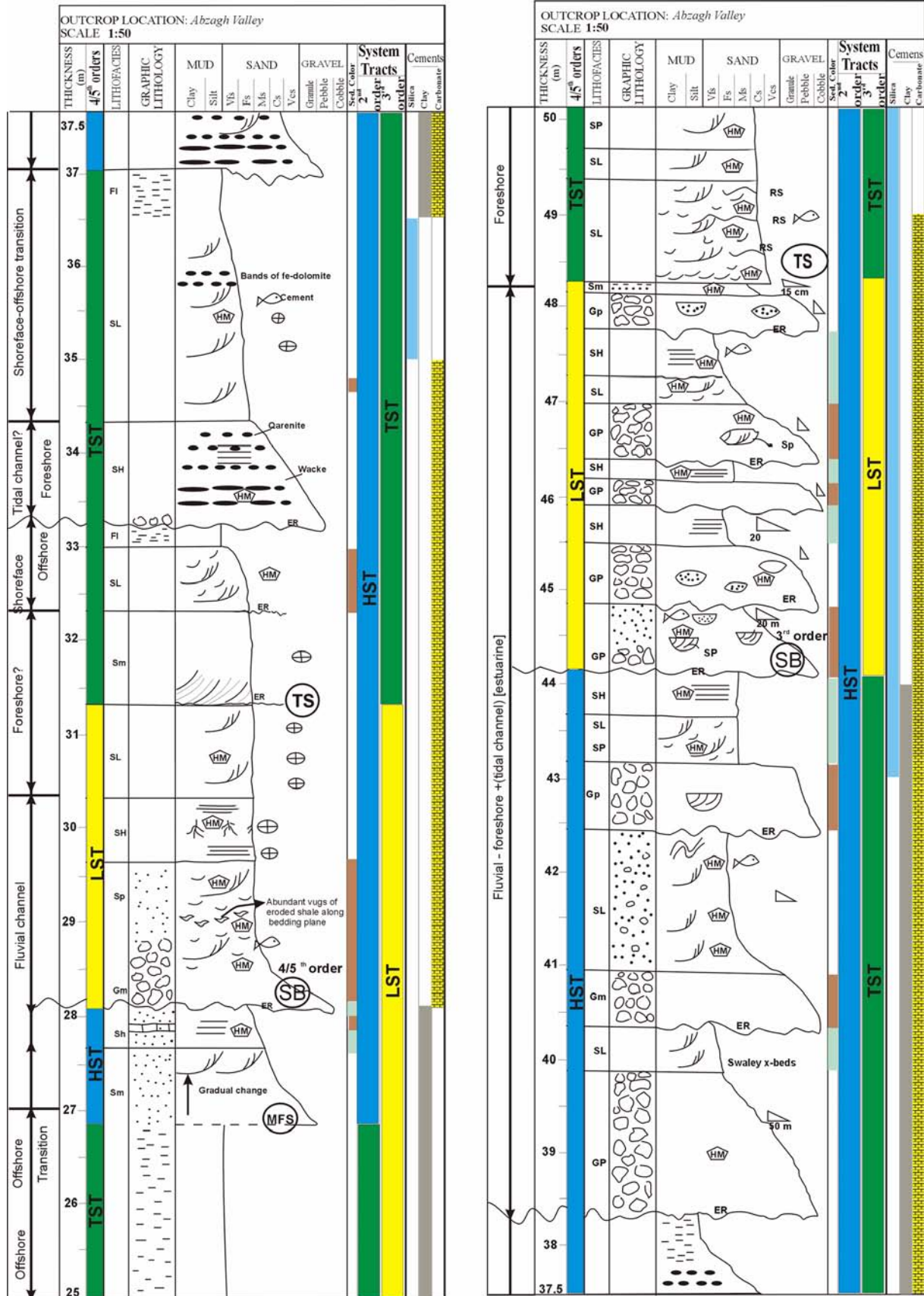


Fig. 2. (continued).



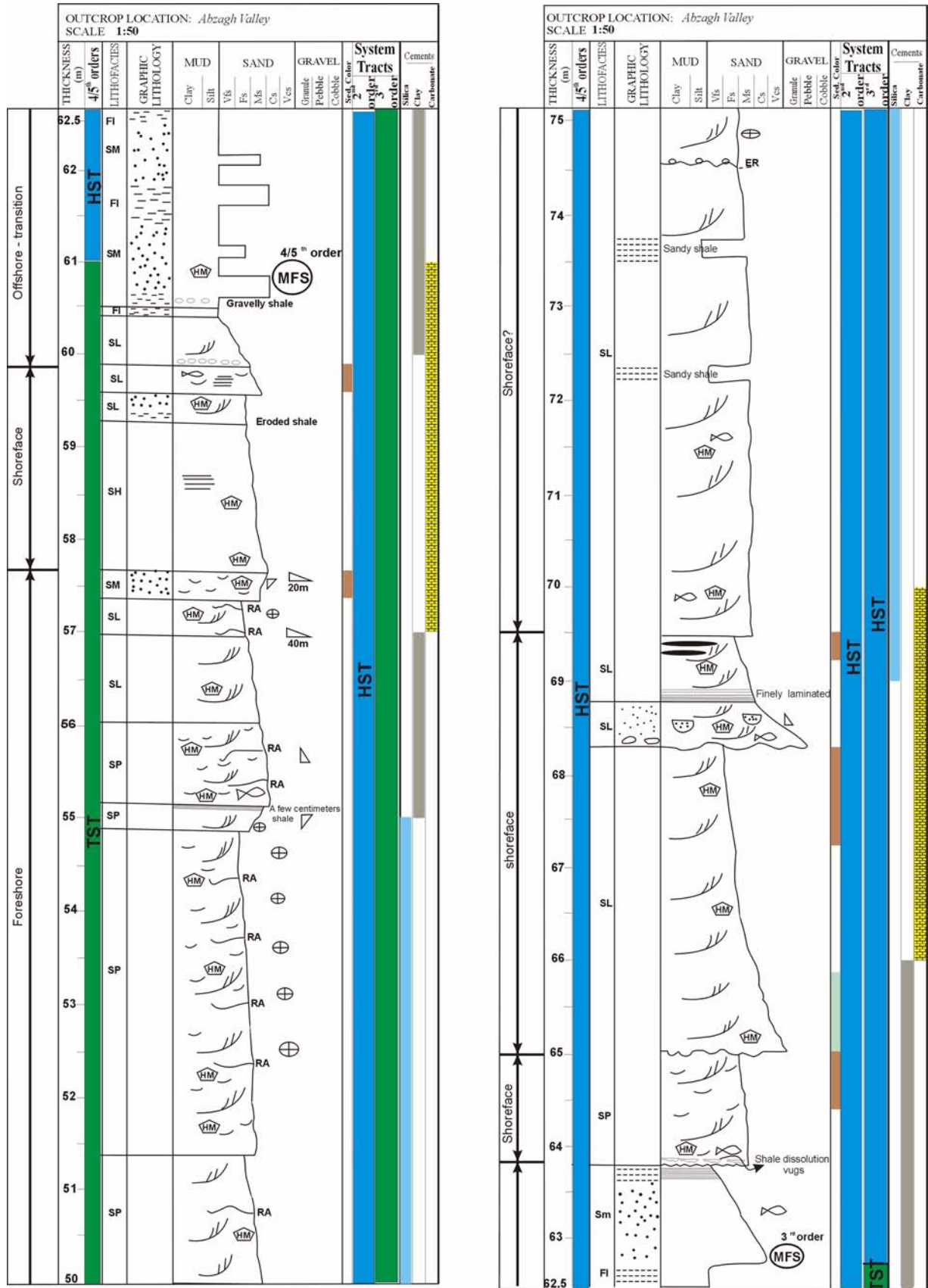


Fig. 2. (continued).

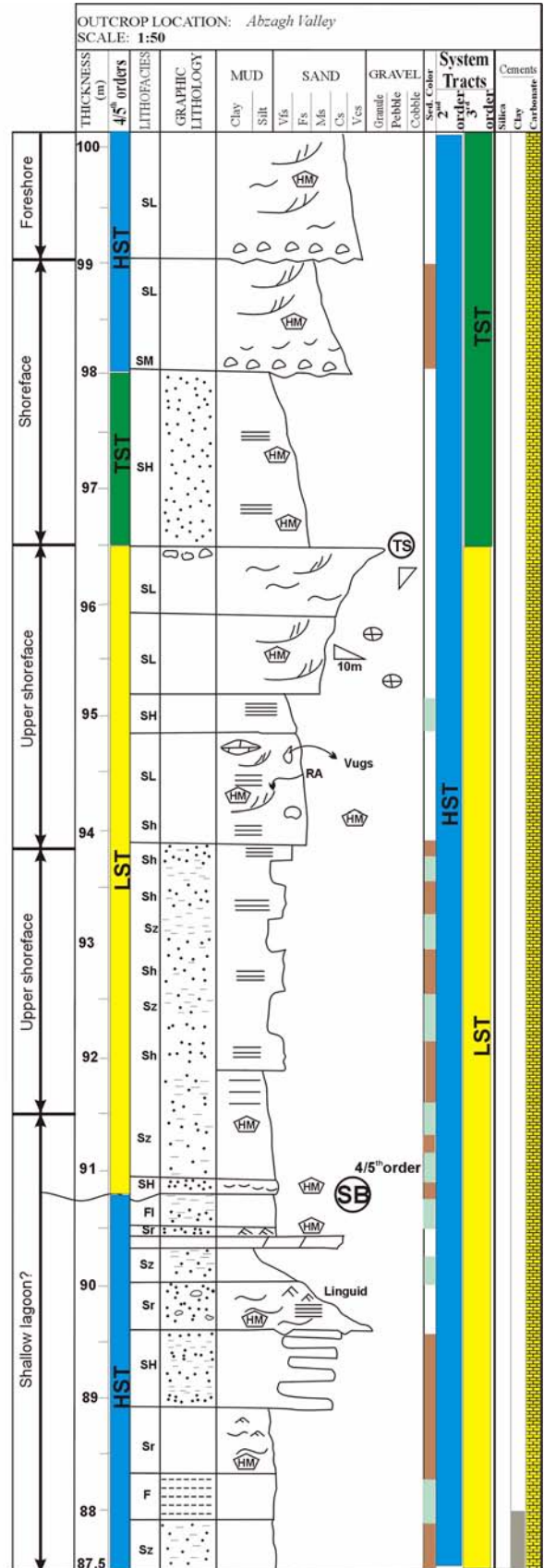
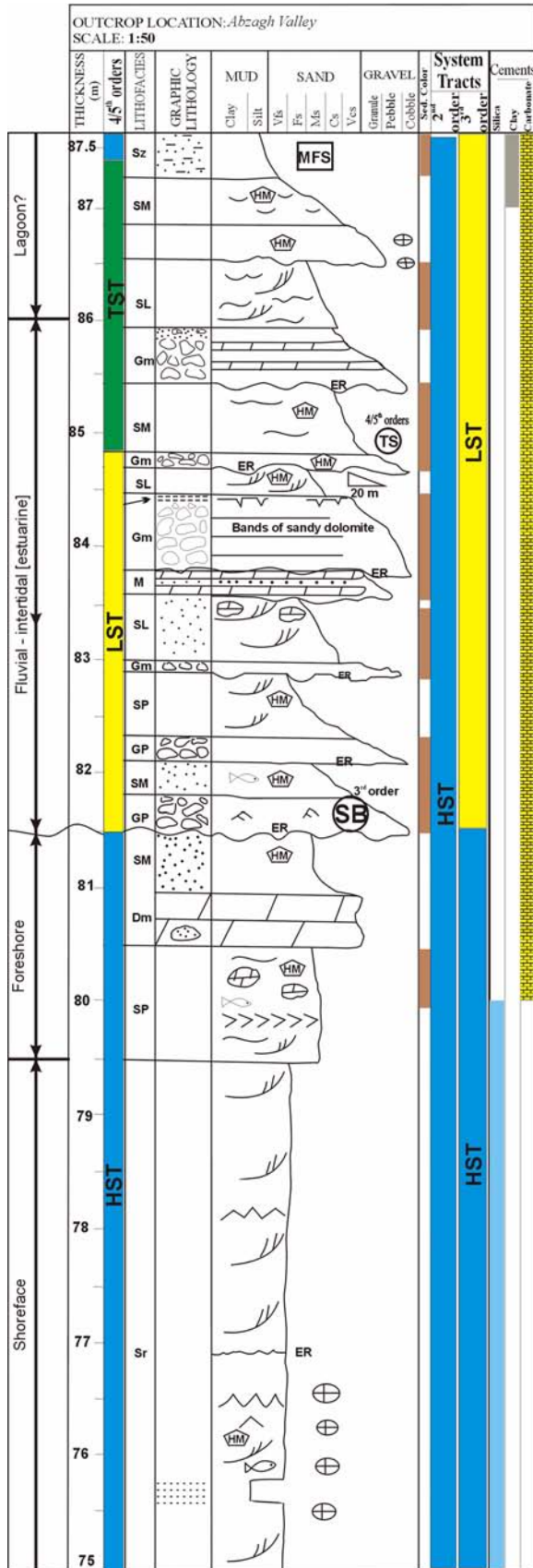


Fig. 2. (continued).

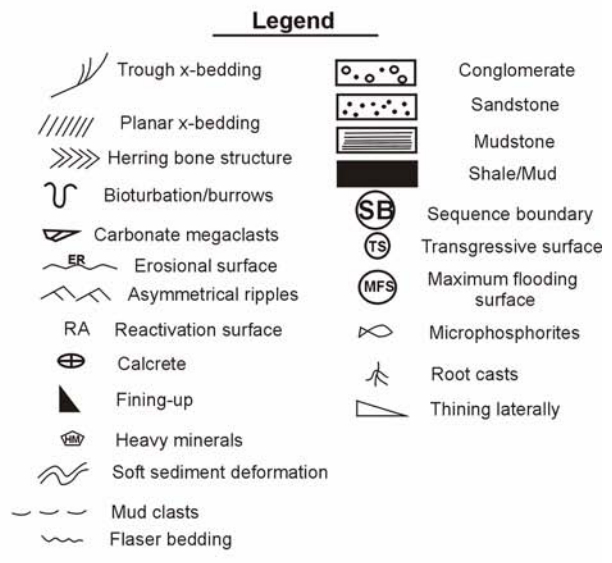
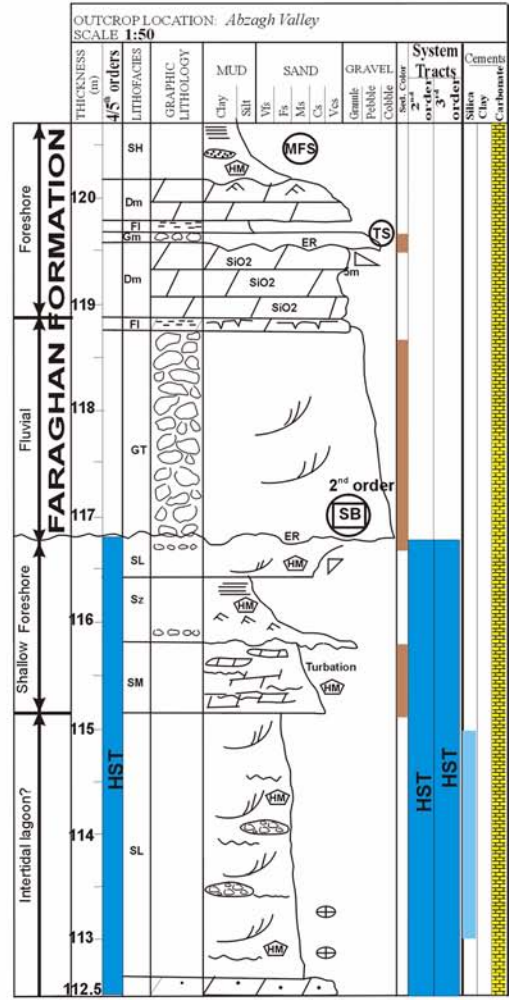
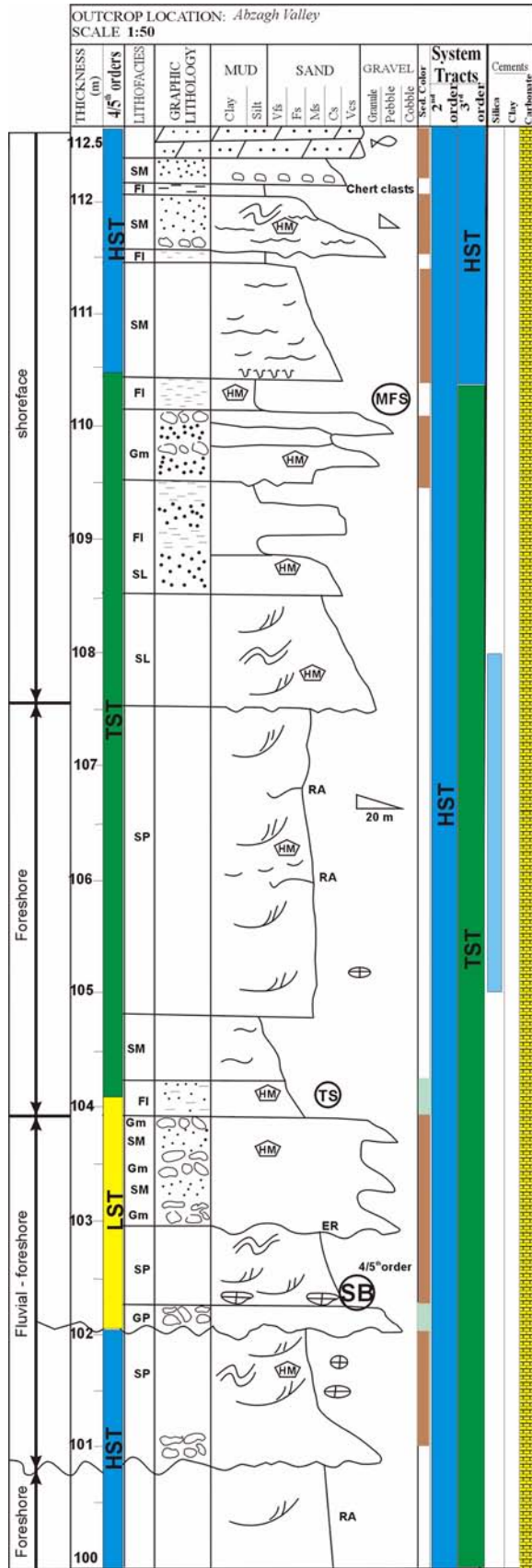


Fig. 2. (continued).



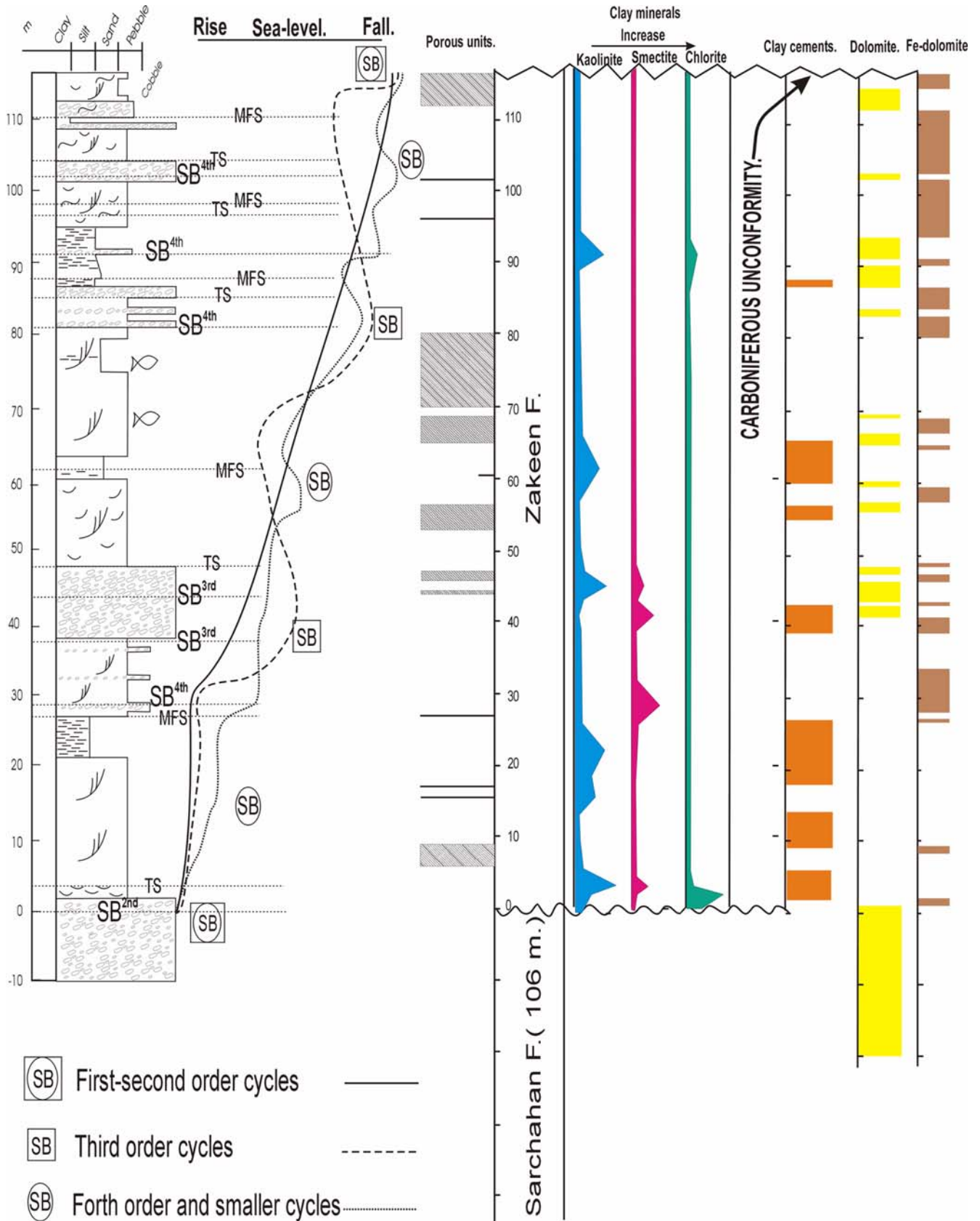


Fig. 3. Distribution pattern of major diagenetic minerals and porous units against systems tracts, sequences, and relative sea-level fluctuation curves.

Diagenetic feature	Early Diagenesis (Eodiagenesis)	Late Diagenesis (Mesodiagenesis) I	Late Diagenesis (Mesodiagenesis) II	Telogenic
Compaction	↔		↔	
Silica cement		↔		
Feldspar authigenesis		↔		
Chlorite cement			↔	
Phosphate cement	←···→			
Dolomite cement	↔		←·····→	←·····→
Fe-dolomite cement	↔			
Zoned Dolomite			←···→ ↔	
Calcite cement	↔		↔ ↔ ←·····→	
Clay minerals	←···→	←·····→	↔	
Fracturing			↔	
Stylolite/Solution seams			←·····→	
Neomorphism		←·····→		
Authigenetic pyrite			←···→	
Feldspar decomposition	↔			←·····→
Fe Oxide				←·····→

↔ Certain occurrence  
 ←·····→ Probable occurrence

Fig. 4. Paragenesis of diagenetic minerals in the Zakeen Formation (Zamanzadeh, 2008).

(Fig. 6). Textural relationship of microcrystalline ferroan dolomite with other diagenetic products (e.g., being engulfed by fine crystalline blocky dolomite or zoned dolomite) shows that it was the first cement phase precipitated in the intergranular porosity (Fig. 5). Preservation of porosity in the cemented sections (Fig. 5), microcrystalline nature of this cement in both forms of stratabound and laterally extensive layers, and high volumetric amount of the cement (about 35% on the average, Table 3) indicate its pre-burial (eogenic) origin (c.f. Taylor et al., 2000). In the studied area, microcrystalline ferroan dolomite cement occurs in the facies related to estuaries, bays and foreshore sub-environments. It is rarely seen in the shoreface and offshore sediments.

Results from oxygen and carbon isotopes measurements on the bulk samples of carbonate cemented rocks reveal a range of 1.06 to -6.00‰ for  $^{18}\text{O}$  and -1.23 to -4.94‰ for  $^{13}\text{C}$  in the Zakeen Formation (Table 4).

## 5.2. Kaolinite and Dickite

Kaolinite with a characteristic vermicular texture (Fig. 7) is found as both pore filling and replacement products of feldspars (Fig. 7). Kaolinite is the most abundant clay mineral identified by XRD and SEM measurements. Some kaolinite crystals show a blocky habit which is typical of dickite (Fig. 7, c.f. Ehrenberg et al., 1993; Morad et al., 1994). The presence of a range of kaolinite platelets and blocky kaolinite in the same sandstone suggests that the kaolinite platelets are the precursor of dickite crystals (c.f. Beaufort et al., 1998; Lanson et al., 2002). Some kaolinite crystals show the incipient growth of illite on them (Fig. 7).

Being both a replacement and the first pore-filling phase, kaolinite (especially the vermicular form) is interpreted as an early diagenetic product formed by flushing shallow-buried sandstones by meteoric-water (Burley and MacQuaker, 1992; De Ros, 1998). Vermicular kaolinite is abundant in sandstones with high feldspar content, i.e., subarkoses and arkoses.

## 5.3. Chlorite Cement

Chlorite cement is frequently observed in some sandstones and conglomerates. It occurs as grain-coating platelets perpendicular to silica overgrowth and as pore-filling patches (Fig. 8). The chlorite cement usually engulfs silica overgrowths, thus postdates the other cement overgrowths. Since it entirely filled the porosity, it has hindered the development of later silica cement precipitation in the pore spaces (Fig. 8). Its occurrence on the silica cement overgrowth, suggests a mesogenetic origin.

## 5.4. Illite-sericite Coating

In petrographic studies, most coatings around detrital grains contain sericite in some extent (Fig. 9). SEM analysis of the same samples reveals that illite is the most abundant clay mineral around the grains (Fig. 9). Due to possible transformation of illite to sericite (K-rich muscovite) (Worden and Morad, 2003) and occurrence of these products together in most cases, the term illite-sericite is preferred here. Illite-sericite coatings usually engulf silica overgrowths, but its temporal relationship with carbonate cements is not clear.

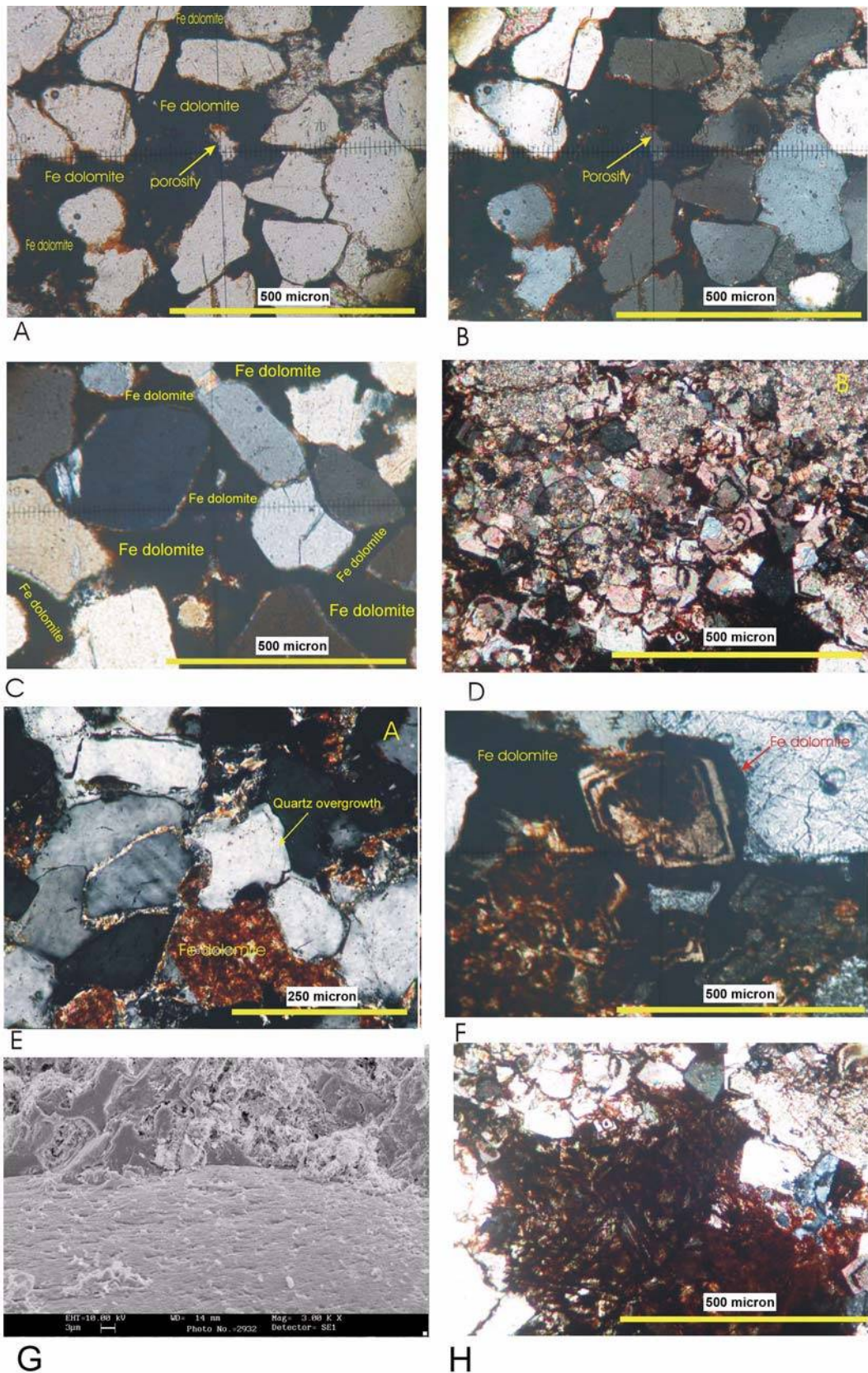


Fig. 5. Different types of ferroan dolomite cement. a-b) Microcrystalline ferroan dolomite with preserved initial porosity in plain polarized and crossed polars respectively, c) High content of early microcrystalline ferroan dolomite, d-f) Recrystallized ferroan dolomite into zoned (d and h) and saddle (f) dolomite, g) SEM image showing early dolomite cement as the first cement precipitating on the grains.



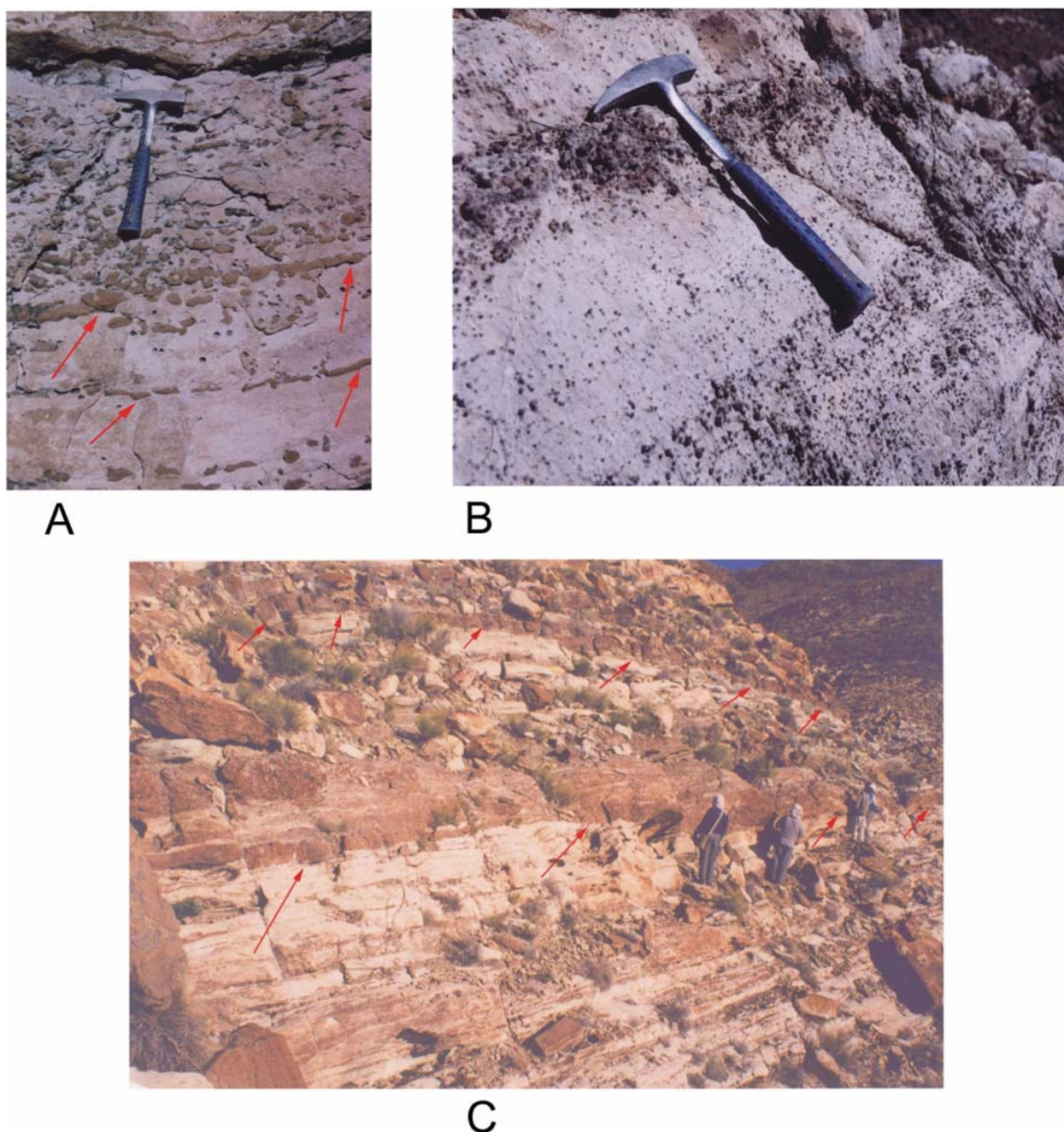


Fig. 6. (a) Laterally extensive layers (arrows) in sandstones, (b) Ferroan dolomite-cemented nodules in sandstones, (c) Laterally extensive ferroan dolomite-cemented conglomerates (arrows).

The coating is very common in studied subarkosic to arkosic sandstone samples. Such association indicates their origination from feldspar alteration. Occurrence of kaolinite along with the illite-sericite coatings in places shows that the kaolinite was the first product resulted from the feldspar alteration during eodiagenesis (Fig. 7). The kaolinite was in turn transformed into sericite (c.f. Pettijohn et al., 1987; Worden and Morad, 2003) in the late stage of mesodiagenesis.

#### 5.5. Phosphate Cement

Phosphate occurs both in the forms of cement and burrow-filling matrix. Some phosphatic lithics, including silt to sand-size intraclasts (fish debris) with phosphatic matrix (microphosphorites of Garzanti, 1991), are also observed (Fig. 10). The phosphate is thought to be from both biogenic (i.e., fish debris or bioclasts) and diagenetic origin. The burrow-filling phosphates, although uncommon, occur

Table 3. Point counting data from highly porous, impregnated with blue-dyed resin (represented with \*) and ferroan-dolomite cemented samples

Sample No.	Grain %	Porosity %
21-1-1*	61.1	38.9
21-1-2*	67.2	32.8
21-1*	60.7	39.3
21-1-3*	73.6	26.4
21-1-4*	67.6	32.4
21-1-5*	65.6	34.4
21-1-6*	56	44
21-1-7*	70	30
21-1-8*	74.4	25.6
21-1-9*	68	32
21-1-10*	73.6	26.4
21-1-11*	67.2	32.8
21-4	53	47
21-4-1	42.3	57.7
21-4-2	59	41
21-4-3	59	41
23-2-1*	58.4	41.6
23-2-2*	64.4	35.6
23-2-4*	46.6	53.4
23-2-5*	49	51
23-2-6*	83.6	16.4
53-1	69.6	30.4
53-10	78	22
53-11	69.6	30.4
53-12	67.4	32.6
53-13	64.6	35.4
53-14	66	34
53-15	62	38
53-16	67.6	32.4
53-17	65.3	34.7
53-18	67.3	32.7
53-19	66.6	33.4
53-21	66.3	33.7
60-1	65.6	34.4
60-5	65.3	34.7
60-7	67	33
60-10	68	32
60-15	63.6	36.4
60-20	66.6	33.4
60-24	67	33
62-1	65	35
62-10	63.6	36.4
62-20	67.3	32.7
62-24	67.3	32.7
113	61.6	38.4
113-1	63	37
113-10	67.3	32.7
113-15	64	36
113-20	67.3	31.7
113-22	53.3	46.7

along flooding surfaces (transgressive surface and maximum flooding surface). The microphosphorites occur in the lower parts of LST and HST deposits.

### 5.6. Quartz and Feldspar Overgrowths

Silica cement occurs in euhedral syntaxial form around quartz grains as overgrowths. Diagenetic quartz occurs in varied amounts in sandstones of all systems tracts. In sandstones, quartz overgrowth is ubiquitously seen filling the remained porosity among the grains with concave-convex contacts. This clearly shows that the sandstones underwent burial and rearrangement of grains before pervasive silica cementation. It shows no obvious distribution pattern related to facies or sequence stratigraphy due to its development in a late stage burial setting. Quartz overgrowths, in the absence of carbonate cements, are the first diagenetic products lying directly on detrital quartz and feldspar grains (Fig. 11). They are usually engulfed by chlorite cement and sericitic coatings.

Diagenetic feldspar overgrowths are minor constituents in sandstones particularly in arkoses. They occur as less than 10 micron K-feldspar and albite overgrowths around detrital feldspar grains as mesogenetic cement. Diagenetic feldspars show no obvious distribution pattern in relation to facies or sequence stratigraphy.

### 5.7. Calcite Cements

Calcite cements are very rarely seen as diagenetic product both in carbonate and clastic rocks. It is observed as very fine crystalline calcite cement lying immediately on carbonate grains such as intraclasts. This type of calcite is rarer than the other types. The other types of calcite cement, include large crystalline blocky and occasionally poikilotopic calcite cements. The blocky calcite fills the large pores especially in conglomerates and fractures in the sandstones and the poikilotopic calcite encompasses carbonate and clastic grains especially in sandstones. The coarse crystalline calcite (blocky and poikilotopic) are considered as mesogenetic cements, especially due to filling the fractures, and the former form (very fine crystalline) as eogenetic cement in the studied rocks.

### 5.8. Diagenetic Porosity

Porosity in the studied rocks varies between zero (in some quartzites) to around 30% (in some subarkoses) (Fig. 12). Minus-cement porosity, particularly in ferroan dolomite-cemented sandstones, reaches up to 57% (Fig. 12; Table 3). Intergranular (primary) and intragranular/dissolution (secondary) are two major types of porosity observed. Development of pervasive secondary porosity in the sandstones sometimes has caused significant erosional features

Table 4. Ferroan dolomite isotopic signatures. All data are relative to VPDB

Samples	Environment	Systems Tract	$^{13}\text{C}$ (‰VPDB)	$^{18}\text{O}$ (‰VPDB)
12-1	Foreshore	TST#1	-2.63	-3.28
20-1	Offshore transition	HST#1	-3.60	-3.13
21-2	Estuarine	LST#2	-2.99	1.06
23-1	Estuarine/Foreshore	LST#2	-3.38	-2.67
60	Shoreface	HST#2	-4.31	-3.05
76	Estuarine	LST#3	-2.46	-3.08
84	Estuarine	LST#3	-4.94/-4.91	-5.90/-6.00
106	Foreshore	LST#3	-1.23	-3.39
155	Foreshore/Lagoon	LST#4	-3.07	-3.93

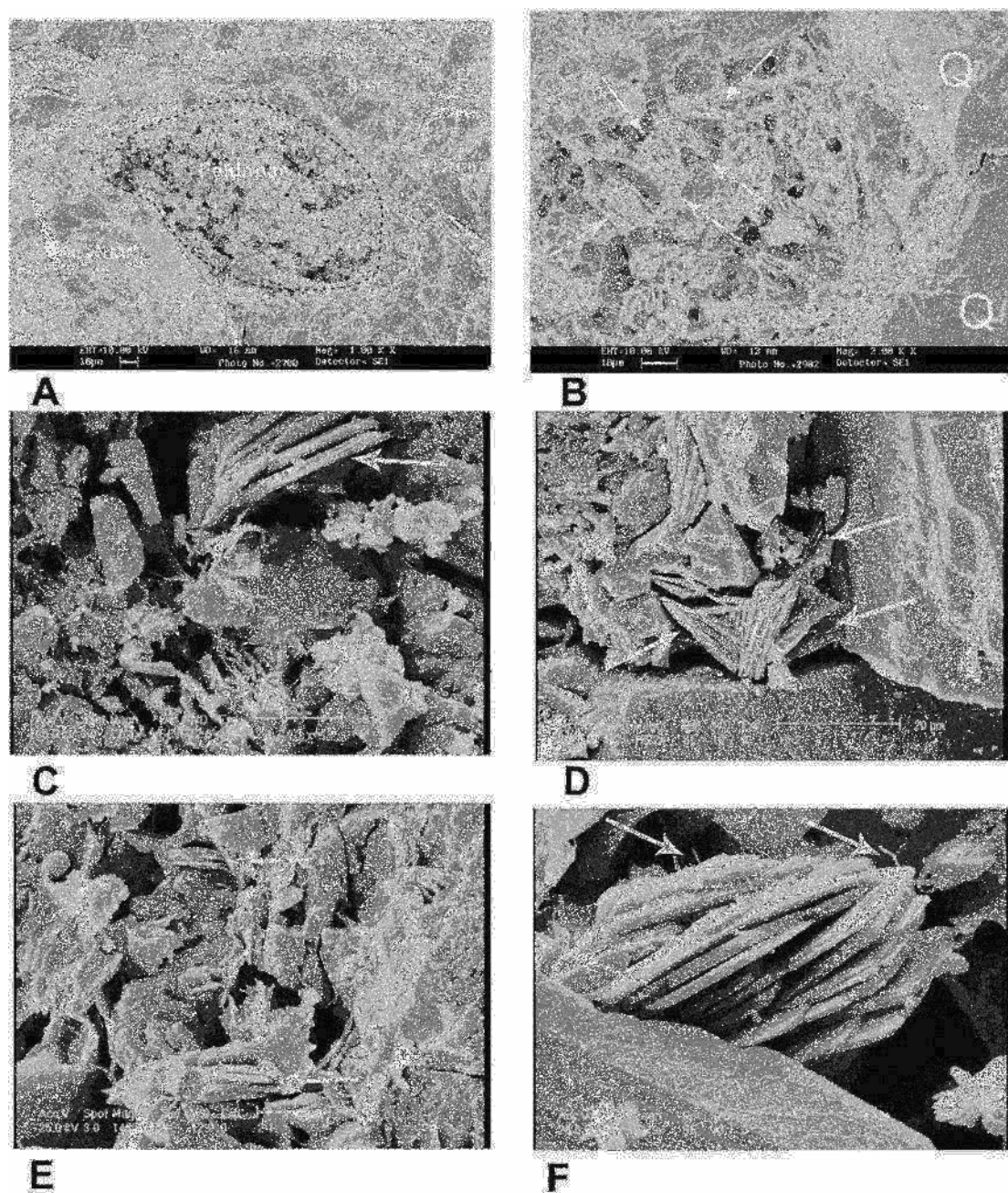


Fig. 7. SEM images showing: (a) Altered feldspar among quartz grains, (b) Growth of vermicular kaolinite (the arrows) within an altered feldspar (Q: quartz), (c-e) incipient growth of dickite crystals (arrows), f) incipient growth of illite crystals (arrows) on kaolinite.



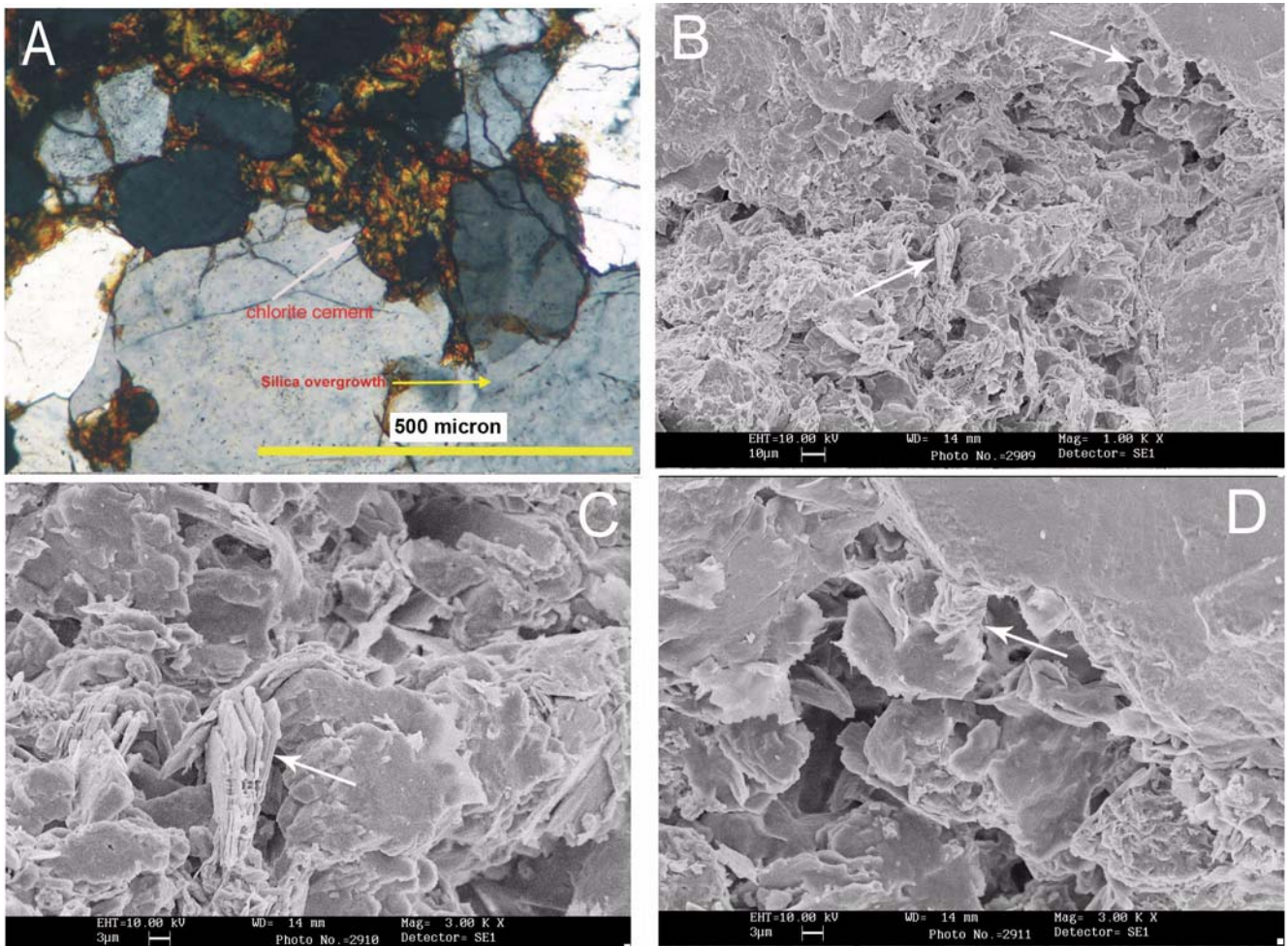


Fig. 8. (a) Photomicrograph showing patches of chlorite cement in sandstone with evident concave-convex contact between quartz grains (crossed polars), (b-d) SEM images of chlorite cement (arrows) grown in the void, perpendicular to the grains surface.

so that leaching carbonate cement (mostly dolomite) of sandstones below unconformities caused loosening of sand grains and development of large cavities during later stages such as telodiagenesis or when the stars cropped out. These features (cavities) are easily seen in the outcrops while the other well cemented strata (e.g., silica cemented ones) are intact. Petrographic studies show that development of the secondary porosity (as dominant type) is mainly due to alteration of feldspar grains and leaching of carbonate cements (mostly dolomite) (Fig. 12).

## 6. DISCUSSION

Distribution pattern of the minerals on the sedimentological logs show close association of ferroan dolomite cements with stratal surfaces, systems tracts and sequences (Fig. 3). Distribution of eogenetic ferroan dolomites was found particularly useful in the discrimination of genetically related facies (parasequences, systems tracts and sequences) and major stratal surfaces (sequence boundary, transgressive

surfaces and maximum flooding surfaces) (e.g., Morad et al., 2000; Taylor et al., 1995, 2000).

Distribution of ferroan dolomite in the sequence stratigraphic framework shows that it is abundant in LST (conglomerates), common in TST, but rare in HST (sandstones) (Figs. 3 and 13). It is strongly associated with flooding surfaces (transgressive and maximum flooding surfaces). Such an association shows that its development was controlled by sediment influx into the basin. In the foreshore and upper shoreface sub-environments, ferroan dolomite was precipitated near sediment-water interface (in pre-existing sediments) during low sediment supply. Longer residence of deposits at sediment-water interface (longer period of low sediment influx to the basin) and lower sedimentation rate facilitated greater amounts of ferroan dolomite cementation (c.f. Ketzner et al., 2002). Prolonged suboxic conditions which were promoted during low sedimentation rates (Raiswell, 1987; Gaynor and Scheihing, 1988; Chow et al., 2000) highly affected the marine sediments at parasequence boundaries, maximum flooding surfaces, and transgressive



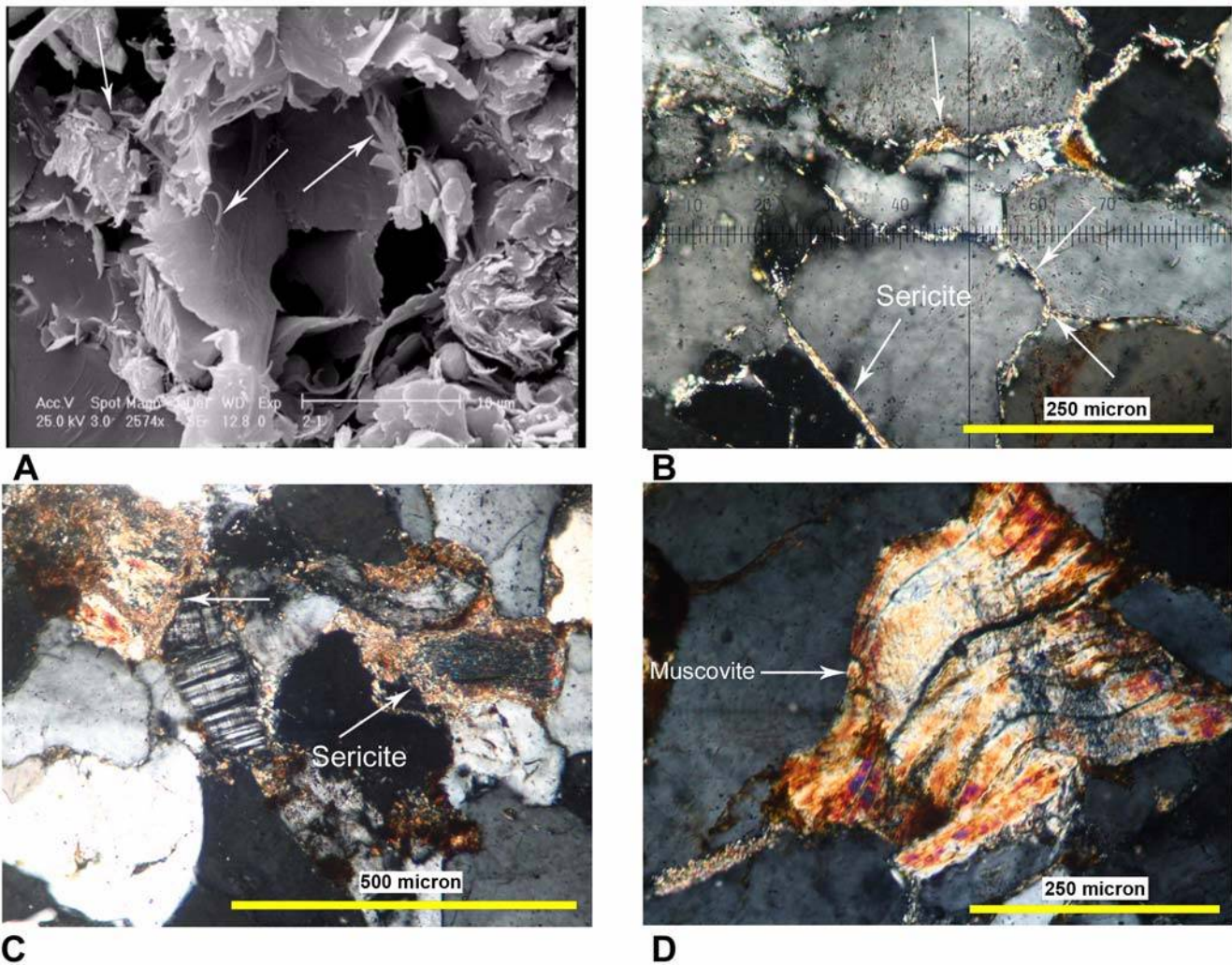


Fig. 9. (a) SEM image showing formation of illite (arrows) from kaolinite, (b-c) Photomicrograph representing illite-sericite coatings (arrows) around clastic grains and on the weathered feldspars (crossed polars), (d) Photomicrograph showing growth of muscovite in the voids (crossed polars).

surfaces (Posamentier and Allen, 1999). In the early stages of relative sea level rise (LST), when sediment supply (S) was nearly equal to accommodation space (A) development (A/S) the pre-existing sediments of LST experienced an extensive ferroan dolomite cementation. In the final stages of rapid sea level rise (TST) where the S/A ratio approached one again (around MFS), the pre-existing deposits of TST experienced similar processes. Development of such diagenetic dolomite was more common in the foreshore and shoreface, which were receiving low/no sediment from the land, though freshwater input was still significant. Decreased clastic and enhanced freshwater input into shallow marine coastal and its sub-environments (estuaries, bays) under warm and equatorial conditions led to dilution of marine pore water. This process inhibited sulfate reduction and incorporation of  $Fe^{2+}$  into sulfides (e.g., Taylor et al., 1995, 2000; Ketzer et al., 2002, 2003). Under such conditions  $Fe^{2+}$

could be absorbed into carbonate cements (Worden and Burley, 2003). Eventually in the early stages of eodiagenesis, ferroan dolomite cement could form and pervasively fill the porosity in sandstones and conglomerates. Formation of microcrystalline ferroan dolomite is ascribed to the presence of modified seawater or brackish water in the reducing nonsulfidic environments (Berner 1981). Such geochemical conditions prevail near the sediment-water interface (~3 cm) in the presence of benthic microbial communities (Wright 2000).

The role of freshwater input in ferroan dolomite development is also understood from oxygen and carbon isotopes measurements (Table 4). The light C and O isotopic signatures explain the role of freshwater influence on ferroan dolomite development. Using the sea water oxygen isotopic signature (Fig. 14) for the Devonian (Veizer et al., 1998; 1999) and the equation presented by Land (1985), the esti-



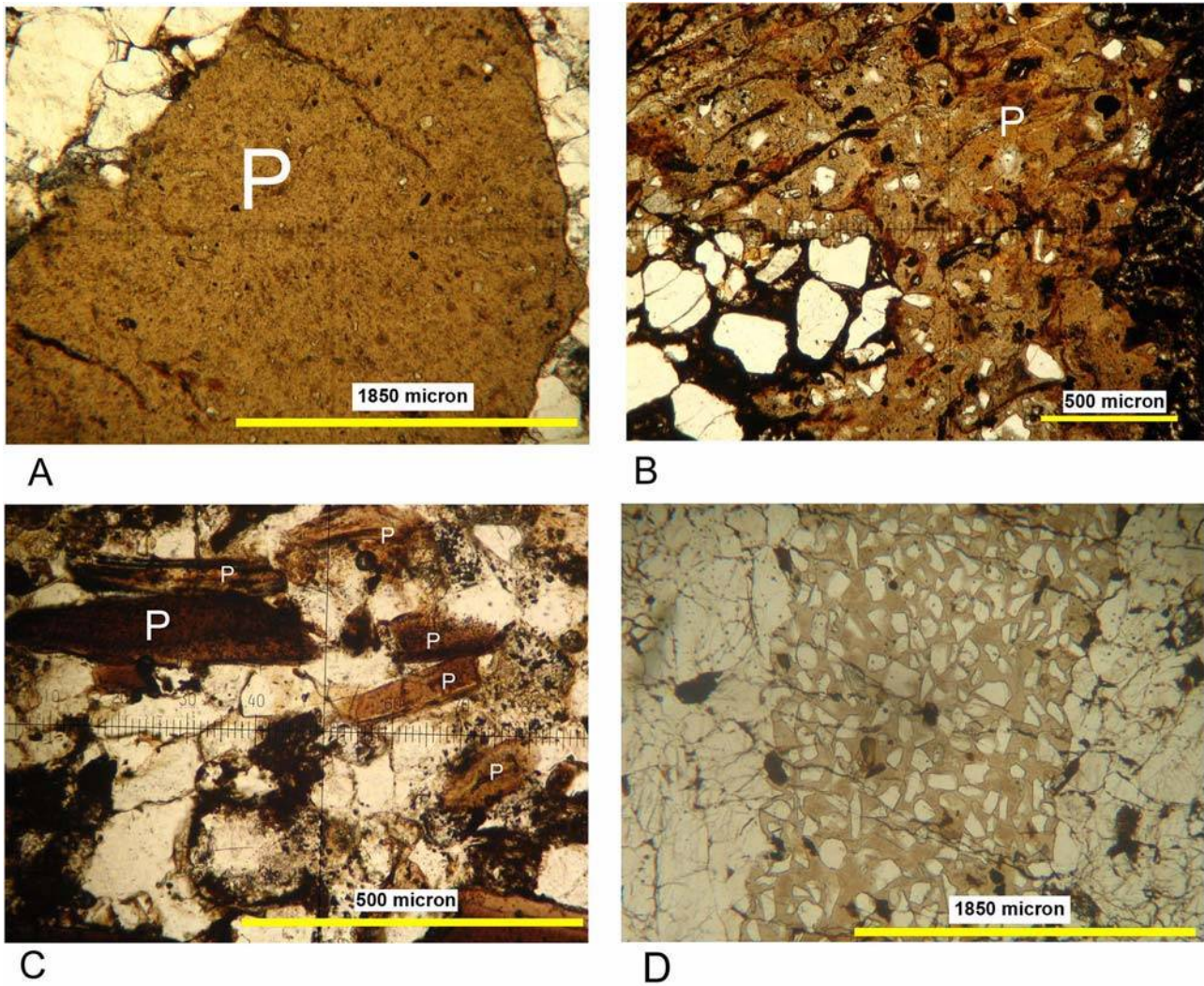


Fig. 10. Phosphatic grains: (a-c) Fish debris and microphosphorites (P: phosphate) (plain polarized), (d) Phosphate-cemented borrows (plain polarized).

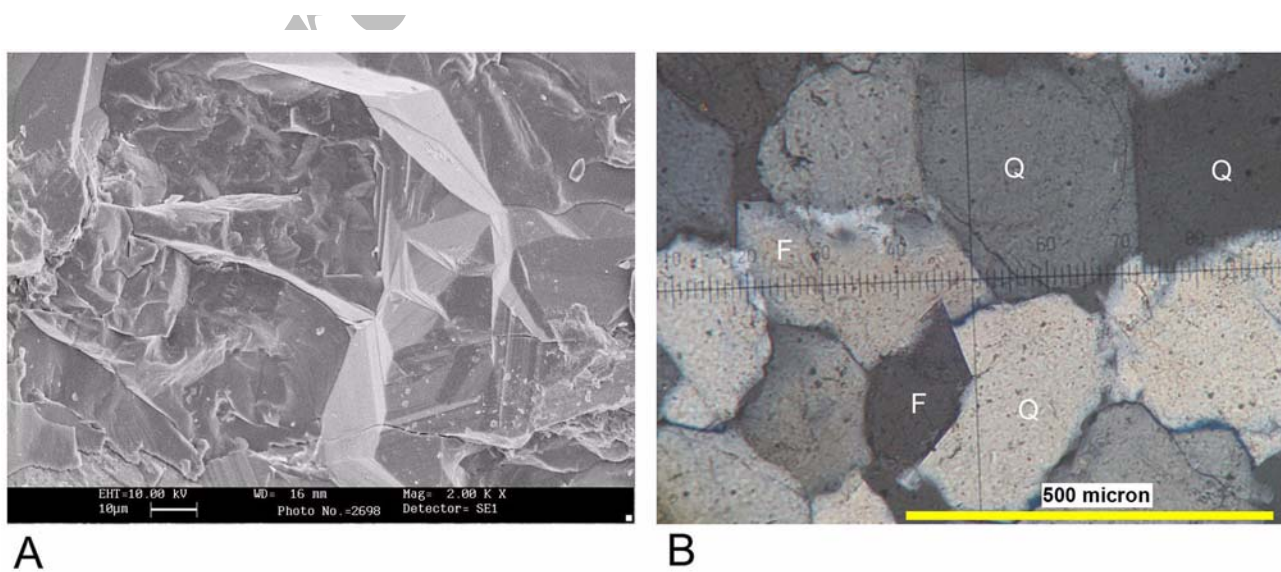


Fig. 11. (a) SEM image of quartz overgrowth, (b) Quartz (Q) and feldspar (F) overgrowths (crossed polars).



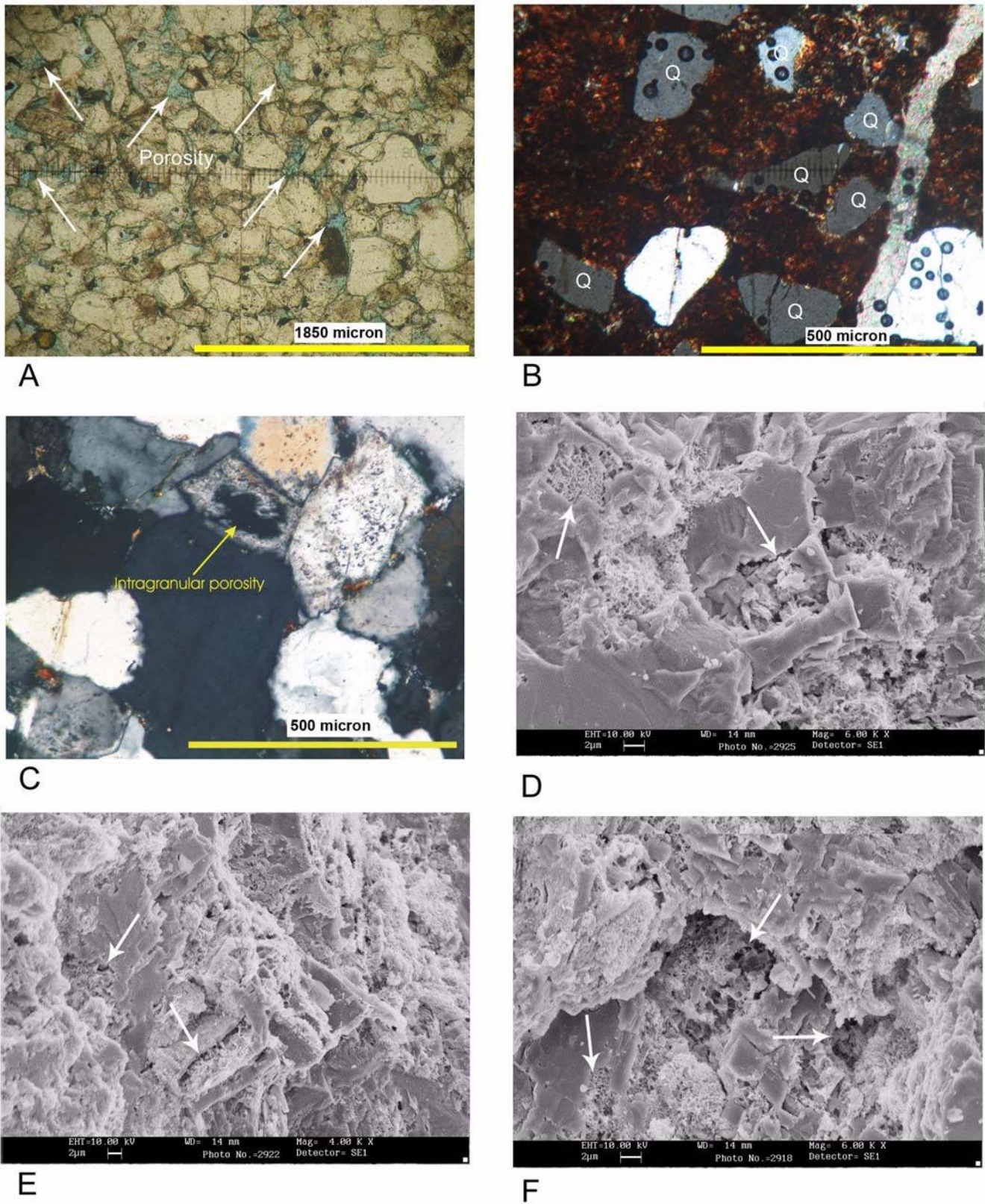


Fig. 12. (a) Intergranular porosity filled with blue-dyed resin (plain polarized), (b) High early dolomite cement content (around 30%, Q: quartz; crossed polars), (c) Secondary intragranular porosity (crossed polars), (d-f) SEM images showing development of secondary porosity resulted from dissolution of dolomite cement (arrows), the voids were later filled with diagenetic products (dolomite and clay minerals).

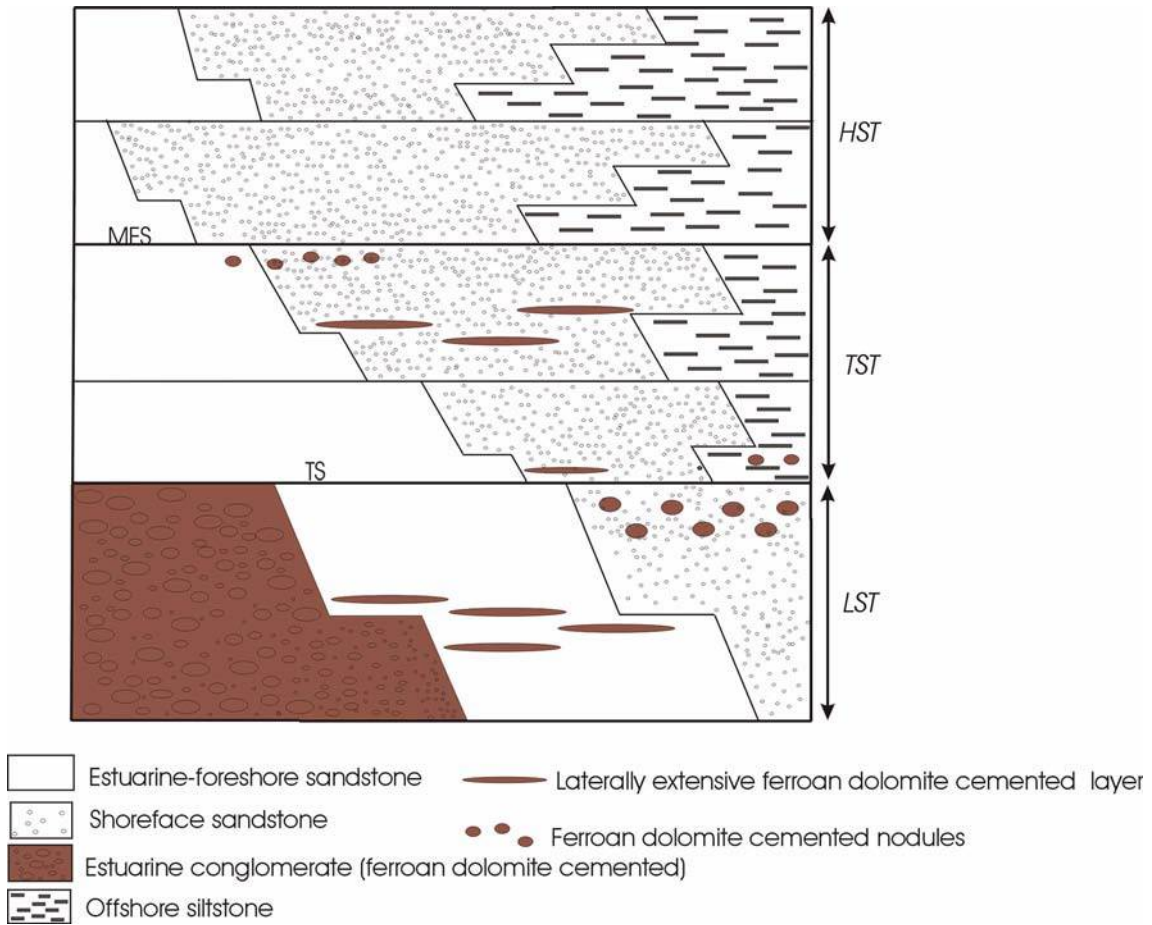


Fig. 13. Schematic distribution of laterally extensive ferroan dolomite layers and nodules in different systems tracts and sedimentary environments in the Zakeen Formation.

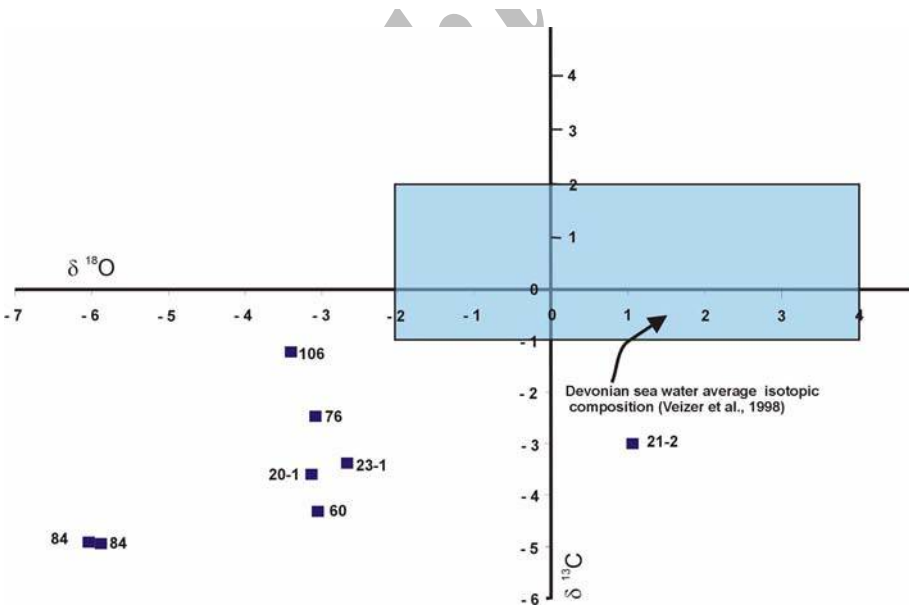


Fig. 14. Scatter diagram showing carbon and oxygen isotopes signatures of analyzed samples against Devonian sea water average oxygen and carbon isotopic signatures (Veizer et al., 1998, 1999).

mated temperature for formation of the ferroan dolomite cement will have a range of 58 to 76 °C. This matches very well with the definition of eogenetic conditions presented by Morad et al. (2000). On the other hand, oxygen isotopic sig-

natures of the ferroan dolomites in the Zakeen Formation falls within the range considered for low temperature dolomites that is -6.50 to +9.00‰ PDB (Allen and Wiggins, 1993). The slightly negative  $^{18}O$  signatures are also con-



sistent with precipitation from modified sea water at slightly elevated temperatures (58-76 °C) associated with sediment shallow burial. The O and C isotopic signatures indicate the influence of mixing of freshwater with marine pore waters on onset of the ferroan dolomite cements development especially in sediments (sandstones) in shallower parts of foreshore where the fresh water input was significant. However, the  $^{13}\text{C}$  and  $^{18}\text{O}$  values and the temperature estimated show that the ferroan dolomite formation started at shallow depth and continued in the eogenetic realm, but its isotopic composition was slightly modified during burial diagenesis. The latter point is well represented by the lighter isotopic signatures of oxygen and carbon (Fig. 14).

The association of sabkha-type micro/fine crystalline dolomite (>10 micron) with supratidal facies shows that prevailing climatic conditions and decrease in clastic input favored its formation. Petrographic evidence clearly shows that the mesogenetic zoned sub-euhedral and saddle dolomites, which always engulf microcrystalline ferroan dolomite, developed during deeper burial and reducing conditions (c.f. McHargue and Price, 1982) of mesogenetic stages (c.f. Mattes and Montjoy, 1980).

Distribution pattern of quartz and feldspar overgrowths,

zoned and saddle dolomite, chlorite and dickite cements and illite-sericite coatings shows no meaningful relation with relative sea-level changes, suggesting that their formation took place in the burial setting. Typical characteristics of deep burial diagenetic products (e.g., saddle dolomites, blocky and poikilotopic calcite, chlorite and illite cements and stylolites) indicate a burial of more than 3000 meters which occurred during the Cretaceous (Fig. 15) for the Zakeen Formation (Zamanzadeh et al., 2006). This is in agreement with burial history diagram proposed for some subsurface sections (Zeinalzadeh, 2000) (Fig. 15). Formation of the mesogenetic minerals (especially saddle dolomite) is suggested to take place in a temperature range of 90-160 °C and dry gas zone condition (Spotl and Pitman, 1998).

The phosphate cement is thought to have been developed in the offshore sub-environment (reduction condition) during relative sea-level rise, when sediment influx to the basin was in the lowest amount (c.f. Amorosi, 1997; Baum and Vail, 1988). Its association with burrowed firm-grounds supports such an idea. The phosphate mostly formed as a cement of newly deposited sediments, some of which underwent the marine erosion later. Such a process is responsible for occurrence of the microphosphorites and

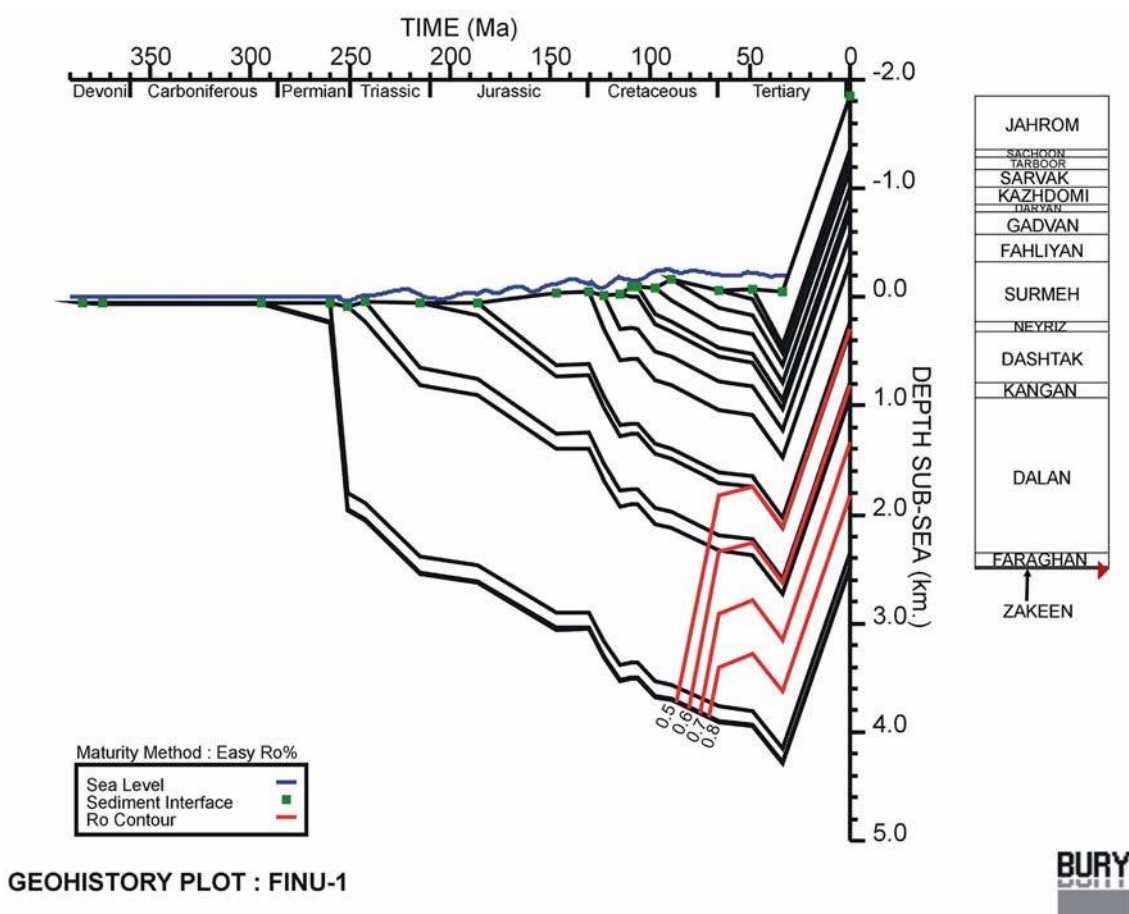


Fig. 15. Burial history diagram of the Zakeen Formation in well finu#1 (Zeinalzadeh, 2000).

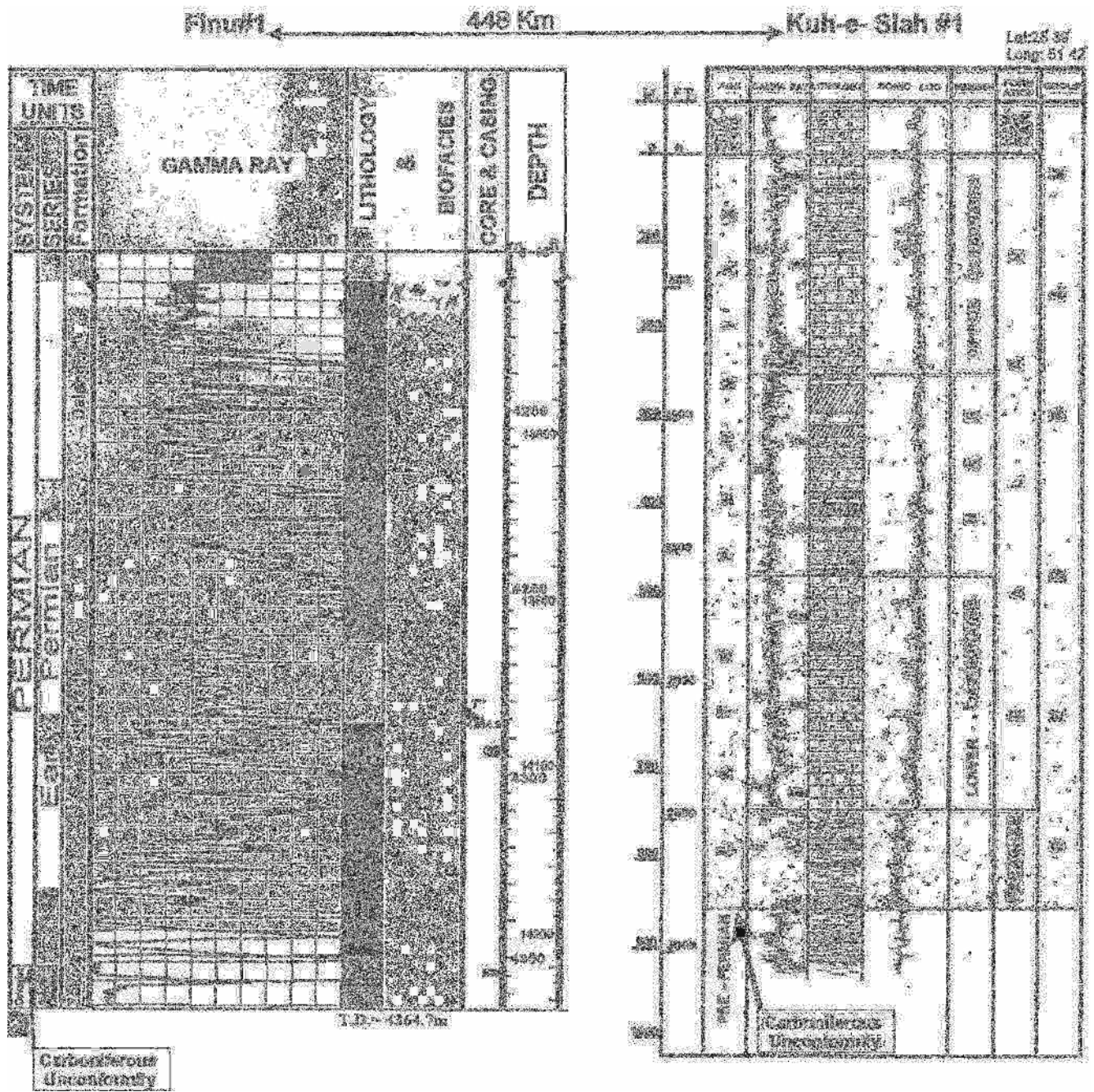


Fig. 16. Electric logs in wells Finu#1 and Ku-e-Siah#1 showing the location of Carboniferous Unconformity represented with abrupt decrease in gamma below the unconformity (modified after Szabo and Kheradpir, 1978).

burrow-filling phosphate in the lower HST deposits (c.f. Kidder and Swett, 1989; Kidwell, 1989; Odin and Letolle, 1980). Phosphate-cemented lithics in the LST deposits, as a type of non-carbonate intraclasts (NCI)-rich arenite (Zuffa, 1980, 1985) may occur between a ravinement surface at the base, which may coincide with an unconformity or a transgressive surface (Baum and Vail, 1988) and a flooding surface at the top (Garzanti, 1991).

Distribution pattern of the porosity on the sedimentological logs (Fig. 3) clearly shows a significant increase below

sequence boundaries. The most porous units occur directly below the major sequence boundary, which separates Devonian from Permian units (Ghavidel-Syooki, 1999). Such increase in the porosity can be well observed on the well-logs, too (Fig. 16). The increase in porosity (interpreted by the abrupt fall in gamma below the Carboniferous unconformity) is related to prolonged subaerial exposure (c.f. Emery et al., 1990) and dissolution of unstable grains and carbonate cements by penetrating meteoric waters. Greater amount of secondary porosity in the foreshore and shore-

face deposits indicates their longer exposure during relative sea-level fall.

## 7. CONCLUSIONS

Diagenetic minerals in the Zakeen Formation comprise two major categories:

(1) Sequence-stratigraphy-related products including ferroan dolomite, sabkha-type dolomite, and phosphate.

(2) Burial related products including quartz and feldspar overgrowths zoned and saddle dolomite, chlorite and illite-sericite (i.e., burial diagenesis products).

Moreover, development of secondary porosity was found a significant sequence-stratigraphy-related phenomenon in the formation. Distribution pattern of the secondary porosity is significantly helpful in discrimination of type 1 (erosional) from type 2 (non-depositional) sequence boundaries. Such results will provide significant information for sequence stratigraphic studies of the formations in the oil fields (sub-surface sections) where cuttings and logs are the only reliable and available data.

Both depositional conditions and sediment influx affected ferroan dolomite cement development in the rocks. So that, the cement was developed in the shallower parts of fore-shore and less frequently in shoreface sub-environments during low sediment influx, when fresh water input to the basin was significant.

Various origin of silica and feldspar overgrowth and their development in different stages of diagenesis minimize their usage in sequence stratigraphic analysis of the formation.

A distinct hiatus (indicated by palynological studies) between the Zakeen (Middle to Upper Devonian) and Faraghan (Lower Permian) formations can be inferred from sequence stratigraphic studies and diagenetic products distribution (Figs. 3 and 16).

**ACKNOWLEDGMENTS:** We express our deep gratitude to the Exploration Manager of the National Iranian Oil Company (NIOC) for their kind assistance and provision of facilities for fieldwork. Thanks are expressed to Ali Mobasheri, Arsalan Bakhshi and Mohammad Reza Naeji from NIOC for their assistance in the field studies. We acknowledge Mohammad Ali Barghi for providing XRD analyses, Mohsen Ranjbaran for his useful comments in petrography studies and S.Morteza Zamanzadeh for his help in graphic works. Professor Sadoon Morad from Upsala University and Dr. Brian Horton from UCLA are highly acknowledged for constructional reading of the manuscript and their useful comments. We also express our gratitude to Dr. Bokyun Ko and two anonymous referees who made precise reviews which helped us in enhancement of final version.

## REFERENCES

Aali, J., Rahimpour-Bonab, H., and Kamali, M.R., 2006, Geochemistry and origin of the world's largest gas field from Persian Gulf, Iran. *Journal of Petroleum Science and Engineering*, 50, 161–175.

Al-Aasm, I., Taylor, B.E., and South, B., 1990, Stable isotope anal-

ysis of multiple carbonate samples using selective acid extraction. *Chemical Geology (Isotope Geoscience Section)*, 80, 119–125.

Alavi, M., 2004, Regional stratigraphy of the Zagros fold-thrust belt of Iran and its proforeland evolution. *American Journal of Science*, 304, 1–20.

Al-Laboun, A.A., 1990, The Paleozoic succession and the influence of Hercynian equivalent movements in the Greater Arabian Basin. *Journal of King Abdulaziz University Earth Science*, 3, 201–215.

Allan, J.R. and Wiggins, W.D., 1993, Dolomite Reservoirs: Geochemical Techniques for Evaluating Origin and Distribution. American Association of Petroleum Geologists Continuing Education Course Note Series, No. 36.

Al-Ramadan, K., Morad, S., Proust, J.N., and Al-Aasm, I., 2005, Distribution of diagenetic alterations in siliciclastic shoreface deposits within a sequence stratigraphic framework: evidence from the Upper Jurassic, Boulonnais, NW France. *Journal of Sedimentary Research*, 75, 943–959.

Al-Sharhan, A.S. and Nairn, A.E.M., 1997, Sedimentary basins and petroleum geology of the Middle East. Elsevier Science B.V., Amsterdam, 843 p.

Amorosi, A., 1995, Glaucony and sequence stratigraphy: conceptual framework of distribution in siliciclastic sequences. *Journal of Sedimentary Research*, B65, 419–425.

Amorosi, A., 1997, Detecting compositional, spatial and temporal attributes of glaucony: a tool for provenance research. *Sedimentary Geology*, 109, 135–153.

Baum, G.R. and Vail, P.R., 1998, Sequence stratigraphic concepts applied to Paleogene outcrops, Gulf and Atlantic basins. In: Wilgus, C.K., Hastings, B.S., Kendall, C.G., St. C., Posamentier, H.W., Ross, C.A., and Van Wagoner, J.C. (eds.), *Sea-Level Changes: an Integrated Approach*. SEPM Special Publication, 42, 309–327.

Beaufort, D., Cassagnabere A., Petit, S., Lanson, B., Berger, G., Lachapagne, J.C., and Johansen, H., 1998, Kaolinite-to-dickite conversion series in sandstone reservoirs. *Clay Minerals*, 33, 297–316.

Berberian, M. and King, G.C.P., 1981, Towards a Paleogeography and tectonic evolution of Iran. *Canadian Journal of Earth Sciences*, 18, 210–265.

Berner, R.A., 1981, A new geochemical classification of sedimentary environments. *Journal of Sedimentary Petrology*, 51, 359–365.

Beydoun, Z.R., 1988, *The Middle East: Regional geology and petroleum resources*. Scientific Press, Beaconsfield, England, 292 p.

Burley, S.D. and Macquaker, J.H.S., 1992, Authigenic clays, diagenetic sequences and conceptual diagenetic models in contrasting basin-margin and basin center North Sea Jurassic sandstones and mudstones. In: Houseknecht, D.W. and Pittman, E.D. (eds.), *Origin, Diagenesis and Petrophysics of Clay Minerals in Sandstones*. SEPM Special Publication, 47, 81–110.

Catuneanu, O., 2002, Sequence stratigraphy of clastic systems: Concepts, merits, and Pitfalls. *Journal of African Earth Sciences*, 35, 1–43.

Chow, N., Morad, S., and Al-Aasm, I., 2000, Origin of authigenic Mn-Fe carbonates and pore-water evolution in marine sediments: evidence from Cenozoic strata of the Arctic Ocean and Norwegian-Greenland Sea (ODP Leg 151). *Journal of Sedimentary Research*, 70, 682–699.

De Ros L.F., 1998, Heterogeneous generation and evolution of diagenetic quartzarenites in Silurian-Devonian Furnas Formation of the Parana' Basin, southern Brazil. *Sedimentary Geology*, 116, 99–128.

Dickinson, W.R., 1970, Interpreting detrital modes of graywacke and

- arkose. *Journal of Sedimentary Petrology*, 40, 695–707.
- Dutton, S.P. and Willis B.J., 1998, Comparison of outcrop and sub-surface sandstone permeability distribution, Lower Cretaceous Fall River Formation, South Dakota and Wyoming. *Journal of Sedimentary Research*, A68, 890–900.
- Ehrenberg S.N., Aagaard P., Wilson M.J., Fraser A.R., and Duthie D.M.L., 1993, Depth-dependent transformation of kaolinite to dickite in sandstones of the Norwegian continental shelf. *Clay Minerals*, 28, 325–352.
- Emery, D., Myers, K.J., and Young, R., 1990, Ancient subaerial exposure and freshwater leaching in sandstones. *Geology*, 18, 1178–1181.
- Frakes, L.A., Francis, J.E., and Syktus, J.T., 1992, *Climate modes of the Phanerozoic*. Cambridge University Press, Cambridge, 286 p.
- Garzanti, E., 1991, Non-carbonate intrabasinal grains in arenites: their recognition, significance, and relationship to eustatic cycles and tectonic setting. *Journal of Sedimentary Petrology*, 61, 959–975.
- Gaynor, G.C. and Scheihing, M.H., 1988, Shelf depositional environments and reservoir characteristics of the Kuparuk River Formation (Lower Cretaceous), Kuparuk Fiel, North Slope, Alaska. In: Lomand, A.J. and Harris, P.M. (eds.), *Giant Oil and Gas Fields: a core workshop*. SEPM Core Workshop, 12, 333–389.
- Ghavidel-Syooki, M., 1986, Palynological study and age determination of Faraghan Formation in Kuh-e-Gahkum region at southeast of Iran. *Iranian Journal of Science and Technology*, 1–2, 11–28.
- Ghavidel-Syooki, M., 1997a, Palynostratigraphy of the Early Permian strata in the Zagros Basin, Southeast-Southwest Iran. *Iranian Journal of Science and Technology*, 18, 243–261.
- Ghavidel-Syooki, M., 1999, Investigation on the Upper Paleozoic strata in Tang-e Zakeen and introducing Zakeen Formation, Kuh-e-Faraghan Zagros Basin, Southern Iran. *Geological Survey of Iran, Geoscience Quarterly Journal*, 29–30, 54–73.
- Ghavidel-Syooki, M., 2003, Palynostratigraphy of Devonian sediments in the Zagros Basin, Southern Iran. *Reviews of Palaeobotany and Palynology*, 127, 241–268.
- Ghavidel-Syooki, M. and Winchester-Seeto, T., 2004, Chitinozoan biostratigraphy and paleogeography of lower Silurian strata (Sar-chahan Formatio) in the Zagros Basin of southern Iran. *Memoirs of the Association of Australasian Paleontologists*, 29, 161–182.
- Husseini, M.I., 1992, Upper Paleozoic Tectono-Sedimentary Evolution of the Arabian and Adjoining Plates. *Geological Society of London*, 149, 419–429.
- Kamali, M.R. and Rezaee, M.R., 2003, Burial history reconstruction and thermal modelling at Kuh-e Mond, SW Iran. *Journal of Petroleum Geology*, 26, 415–46.
- Kashfi, M.S., 1992, Geology of the Permian “supergiant” gas reservoirs in the greater Persian Gulf area. *Journal of Petroleum Geology*, 15, 465–480.
- Ketzer, J.M., Morad, S., and Amorosi, A., 2003, Predictive diagenetic clay-mineral distribution in siliciclastic rocks within a sequence stratigraphic framework. In: Worden R. and Morad, S. (eds.), *Clay Mineral Cements in Sandstones*, International Association of Sedimentologists Special Publication, 34, 42–59.
- Ketzer, J.M., Morad, S., Evans, R., and Al-Aasm, I.S., 2002, Distribution of diagenetic alterations in fluvial, and shallow marine sandstones within a sequence stratigraphic framework: evidence from Mullagmore Formation (Carboniferous), NW Ireland. *Journal of Sedimentary Research*, 72, 760–774.
- Kidder, D.L. and Swett, K., 1989, Basal Cambrian reworked phosphates from Spitsbergen (Norway) and their implications. *Geological Magazine*, 126, 79–88.
- Kidwell, S.M., 1989, Stratigraphic condensation of marine transgressive records: origin of major shell deposits in the Miocene of Maryland. *Journal of Geology*, 97, 1–29.
- Konert, G., Afifi, A.M., Al-Hajri, S.A., and Droste, H.J., 2001, Paleozoic Stratigraphy and Hydrocarbon Habitat of the Arabian Plate. *GeoArabia*, 6, 407–442.
- Land, L.S., 1985, The origin of massive dolomite. *Journal of Geological Education*, 33, 112–125.
- Lanson, B., Beaufort, D., Berger, G., Bauer, A., Cassagnabère, A., and Munnier, A., 2002, Authigenic kaolin and illitic minerals during burial diagenesis of sandstones: a review. *Clay Minerals*, 31, 1–22.
- Loomis, J.L. and Crossey, L.J., 1996, Diagenesis in a cyclic, regressive siliciclastic sequence: the Point Lookout Sandstone, San Juan Basin, Colorado. In: Crossey, L.J., Loucks, R. and Totten, M.W. (eds.), *Siliciclastic Diagenesis and Fluid Flow: Concepts and Applications*. SEPM Special Publication, 55, 23–36.
- Mattes, B.W. and Montjoy, E.W., 1980, Burial dolomitization of Upper Devonian Miette buildup, Jasper National Park, Alberta. In: Zenger, D.H., Dunham, J.B., and Ethington, R.L. (eds.), *Concepts and Models of Dolomitization*. SEPM Special Publication, 28, 250–297.
- McGillivray, J.G. and Husseini, M.I., 1992, The Paleozoic petroleum geology of central Arabia. *American Association of Petroleum Geology Bulletin*, 76, 1473–1490.
- McHargue, T.R. and Price, R.C., 1982, Dolomite from clay in argillaceous or shale associated marine carbonates. *Journal of Sedimentary Petrology*, 52, 873–880.
- McKay, J.L., Longstaffe, F.J., and Plint, A.G., 1995, Early diagenesis and its relationship to depositional environment and relative sea-level fluctuations (Upper Cretaceous Marshybank Formation, Alberta and British Columbia). *Sedimentology*, 42, 161–190.
- Miall, A.D., 1985, Architectural element analysis: a new method of facies analysis applied to fluvial deposits. *Earth Science Reviews*, 22, 261–308.
- Miall, A.D., 1999, *Principles of Basin Analysis*. 3<sup>rd</sup> edition, Springer-Verlag, Berlin, 616 p.
- Morad, S., Ben Ismail, H., De Ros, L.F., Al-Aasm, I.S., and Serrhini, N.E., 1994, Diagenesis and formation water chemistry of Triassic reservoir sandstones from southern Tunisia, *Sedimentology*, 41, 1253–1272.
- Morad, S., Ketzer, J.M., and De Ros, L.F., 2000, Spatial and temporal distribution of diagenetic alterations in siliciclastic rocks: implications for mass transfer in sedimentary basins. *Sedimentology*, 47 (Supplement 1), 95–120.
- Moss, S.J. and Tucker, M. E., 1996, Dolomitization associated with transgressive surfaces – a mid Cretaceous example. *Sedimentary Geology*, 107, 11–20.
- Odin, G.S. and Letolle, R., 1980, Glauconitization and phosphatization environments: a tentative comparison. In: Bendor, Y.K. (ed.), *Marine Phosphorites*. SEPM Special Publication, 29, 227–237.
- Pettijohn, F.J., Potter, P.E., and Siever, R., 1987, *Sand and Sandstone*. Springer-Verlag, New York, 553 p.
- Posamentier, H.W. and Allen, G.P., 1999, *Siliciclastic sequence stratigraphy – Concepts and Applications*. SEPM Concepts in Sedimentology and Paleontology Series 7, SEPM, Tulsa, 204 p.
- Raiswell, R., 1987, Non-steady state microbiological diagenesis and the origin of concretions and nodular limestones. In: Marshall, J.D. (ed.), *Diagenesis of sedimentary sequences*, Geological Society of London, Special Publication, 36, 41–54.



- Read, J.F. and Horbury, A.D., 1993, Eustatic and tectonic controls on porosity evolution beneath sequence-bounding unconformities and parasequences disconformities on carbonate platforms. In: Horbury, A.D. and Robinson, A.G. (eds.), *Diagenesis and Basin Development*, American Association of Petroleum Geology studies in Geology, 36, 155–197.
- Reading, H.G., 1996, *Sedimentary Environments: Processes, Facies, & Stratigraphy*. 3<sup>rd</sup> edition, Blackwell Science, Oxford, 704 p.
- Selley, R.C., 1996, *Ancient Sedimentary environments and their subsurface diagnosis*. 4<sup>th</sup> edition, Chapman and Hall, 300 p.
- Smith, A.G., Hurley, A.M. and Briden, J.C., 1981, *Phanerozoic Paleogeographic World maps*. Cambridge Earth Science series, Cambridge University press, Cambridge, 107 p.
- South, D.L. and Talbot, M.R., 2000, The sequence stratigraphic framework of carbonate diagenesis within transgressive fan-delta deposits: Sant Llorenç del Munt fan-delta complex, SE Ebro Basin, NE Spain. *Sedimentary Geology*, 138, 179–198.
- Spotl, C. and Pitman, J.K., 1998, Saddle (baroque) dolomite in carbonates and sandstones: a reappraisal of a burial-diagenetic concept. In: S. Morad (Editor), *Carbonate cementation in sandstones*. Special Publication of International Association of Sedimentologists, 26, 437–460.
- Szabo, F. and Kheradpir, A., 1978, Permian and Triassic stratigraphy, Zagros basin, southwest Iran. *Journal Petroleum Geology*, 1, 57–82.
- Tang, Z., Parnell, J.P., and Ruffell, A.H., 1994, Deposition and diagenesis of the lacustrine-fluvial Cangfengou Group (Uppermost Permian to Lower Triassic), Southern Junggar Basin, NW China: a contribution from sequence stratigraphy. *Journal of Paleolimnology*, 11, 67–90.
- Taylor, K.G., Gawthorpe, R.L., and Van Wagoner, J.C., 1995, Stratigraphic control on laterally persistent cementation, Book Cliffs, Utah. *Journal of Sedimentary Research*, 69, 225–228.
- Taylor, K.G., Gawthorpe, R.L., Curtis, C.D., Marshall, J.D., and Awwiller, D.N., 2000, Carbonate cementation in a sequence stratigraphic framework: Upper Cretaceous Sandstones, Book Cliffs, Utah-Colorado. *Journal of Sedimentary Research*, 70, 360–372.
- Tucker, M.E., 1993, Carbonate diagenesis and sequence stratigraphy. *Sedimentary Reviews*, 1, 51–72.
- Vail, P.R., Mitchum, R.M., Jr., and Thompson, S., 1977, Seismic stratigraphy and global changes of sea level, Part 4, global cycles of relative changes of sea level. In: Payton, C.E. (ed.), *Stratigraphic interpretation of seismic data*, American Association of Petroleum Geologists Memoir, 26, 83–98.
- Veizer, J., Bruckschen, P., Pawellek, F., Diener, A., Podlaha, O.G., Carden, G.A.F., Jasper, T., Korte, C., Strauss, H., Azmy, K., and Ala, D., 1998, Oxygen isotope evolution of Phanerozoic sea water. *Paleogeography, Paleoclimatology, Paleoecology*, 132, 159–172.
- Veizer, J., Ala, D., Azmy, K., Bruckschen, P., Buhl, D., Bruhn, F., Carden, G.A.F., Diener, A., Ebner, S., Godderis, Y., Jasper, T., Korte, C., Pawellek, F., Podlaha, O.G., and Strauss, H., 1999,  $^{87}\text{Sr}/^{86}\text{Sr}$ ,  $^{13}\text{C}$  and  $^{18}\text{O}$  evolution of Phanerozoic seawater. *Chemical Geology*, 161, 59–88.
- Walker, R.G., 1992, Facies, facies models and modern stratigraphic concepts. In: Walker, R.G. and James, N.P. (eds.), *Facies Models*, Geological Association of Canada, 1–14.
- Worden, R. and Burley, S.D., 2003, Sandstone Diagenesis: the evolution of sand to stone. In: Burley, S.D. and Worden R. (eds.), *Sandstone Diagenesis: Recent and Ancient*, International Association of Sedimentologists Reprint Series, 4, 3–46.
- Worden, R.H. and Morad, S., 2003, Clay minerals in Sandstones: Control on formation, distribution and evolution. In: Worden, R. and Morad, S., (eds.), *Clay Mineral Cements in Sandstones*, International Association of Sedimentologists Special Publication 34, 3–41.
- Wright, D.T., 2000, Benthic microbial communities and dolomite formation in marine and lacustrine environments – a new dolomite model. In: Glenn, C.R., Lucas, J., and Lucas, L. (eds.), *Marine Authigenesis: From Global to Microbial*, Society of Economic Paleontologists and Mineralogists Special Publication, 65, 7–20.
- Zamanzadeh, S.M., 2008, Sedimentary petrology/environment and sequence stratigraphy of Zakeen and Faraghan Formations in their type section (Bandar-Abbas area), Ph.D. thesis, University of Tehran, Iran, 350 p. (in Persian).
- Zamanzadeh, S.M., Ghavidel-Syooki, M., and Amini, A.H., 2006, Applying diagenetic products in reconstruction of burial history of Zakeen and Faraghan Formations, Gahkum Mountain. 24<sup>th</sup> National Symposium on geosciences, Geological Society of Iran, p. 284–285.
- Zeinalzadeh, A., 2000, Burial history and thermal modeling of Dehram, Khami and Bangeestan groups in the Fars Area, South Iran. MS. thesis, University of Tehran, Iran, 227 p. (in Persian).
- Zharkov, M.A. and Chumakov, N.M. 2001, Paleogeography and sedimentation settings during Permian-Triassic reorganizations in biosphere. *Stratigraphy and Geological Correlation*, 9, 340–363.
- Zuffa, G.G., 1980, Hybrid arenites: their composition and classification. *Journal of Sedimentary Petrology*, 50, 21–29.
- Zuffa, G.G., 1985, Optical analyses of arenites: influence of methodology on compositional results. In: Zuffa, G.G. (ed), *Provenance of Arenites*, Boston, D. Reidel, p.165–189.

---

Manuscript received March 1, 2008

Manuscript accepted January 31, 2009